TiS Trends in Sciences
TRENDS IN SCIENCES 2027; 24(1): 14282
SPRINT Scholarly Publishing and Repository Integration Center
https://doi.org/10.48048/tis.2027.14282
RESEARCH ARTICLE

In Silico and *In Vivo* Evaluation of Topical Preparations of Red Betel Extract Nanoliposome (*Piper Crocatum*) for the Treatment of Cut Wounds in Mice

Siti Imroatul Maslikah[1,*], Wira Eka Putra[2], Sri Rahayu Lestari[1], Ajeng Daniarsih[1], Agung Witjoro[1], Alif Baroroh[1], Nur Laila[1] and Eka Desi Lilin Yuliani[1]

[1]Department of Biology, Faculty of Mathematics and Natural Sciences, Universitas Negeri Malang, Malang, Indonesia
[2]Biotechnology Study Program, Department of Applied Sciences, Faculty of Mathematics and Natural Sciences, Universitas Negeri Malang, Malang, Indonesia

([*]Corresponding author's e-mail: siti.imroatul.fmipa@um.ac.id)

Received: 4 May 2026, Revised: 15 June 2026, Accepted: 25 June 2026, Published: 10 August 2026

Abstract

This study aims to develop topical red betel extract (*Piper crocatum*) nanoliposomes as a wound-healing agent in mice (*Mus musculus*). An in-silico study demonstrated the potential of red betel compound to inhibit cyclooxygenase-2 and estrogen receptors, which modulate the inflammatory response. Furthermore, red betel ethanol extract was obtained by percolation using 70% ethanol, then formulated into liposomes through thi-layer hydration with phospholipids, cholesterol, and phosphate buffer (pH 7.4). Red betel extract liposomes ointment (LPC) was prepared at concentration of 6%, 9%, and 12% using a lanolin-petroleum base. Physical evaluation included organoleptic, pH, dispersibility, viscosity, and stability test during 28 days of storage. *In vivo* tests were performed on male mice with 1×1 cm stab wounds, which received topical treatment once daily for 14 days. The evaluation results showed that all ointments had a stable semi-solid texture, a pH within the skin's normal range (4.5 - 6.5), and spreadability in the ideal range (5 - 7 cm). The liposome formula demonstrated physical stability without a rancid odor and exhibited emollient-occlusive properties. Increasing liposome levels affected the color of the preparation and enhanced anti-inflammatory activity by modulating inflammatory mediators and reducing oxidative stress. From the test results, LPC9 showed the best physical stability, while LPC12 showed the most optimal wound-healing effects and blood profile improvement. Thus, topical preparations of red betel extract nanoliposome have the potential to be developed as phytopharmaceutical agents for the treatment of incision wounds.

Keywords: *Piper crocatum*, Liposomes, Topical ointments, Incisions, Wound healing

Introduction

Wounds are a common condition characterized by the loss of skin epithelial integrity [1]. In the United States, the prevalence of wounds is approximately 3.50 per 1,000 populations and encompasses various wound types, including incisional wounds. In Indonesia, according to Basic Health Reseach (2018), the prevalence of stab wounds reached 20.1%, with the highest rates reported in Papua (7.74%). Incised wound (vulnus scissum) is caused by sharp objects, such as knives or glass. They are typically characterized by clean, regular wound edges resulting from direct cutting [2].

If not properly managed, incised wounds are highly susceptible to infection due to microbial invasion from endogenous or exogenous source. Symptoms of infection include redness, swelling, increased pain, pus formation, and fever. Therefore, timely wound clouse is essential, particularly during the early phase of healing, to minimize the risk of infection. Various wound management strategies have been developed, including dressing, ointment, and topical agent. Recently, advancement in nanotechnology has introduced promising innovation in wound care. Due to their small particle size, nanocarriers can penetrate target cells more effectively. Drug delivery systems (DDS), such as

liposomes, have been shown to enhance wound healing, reduce side effects, and improve the bioavalability of therapeutic agents. Liposomes and other nanosystems also prolong drug retention at the wound site, enabling controlled release and achieving high local concentration with lower total doses [3,4]. Liposomes, including nanoliposomes, can enhace drug activity and are used in drug delivery and biological membrane studies [5]. Nanoliposomes are nano-sized lipid vesicles formed via hydrophilic-hydrofobic between phospholipids and water molecules [6]. However, maintaining particle size stability remains a challenge due to the aggregation during storage. Natural ingredients such as red betel (*Piper crocatum* Ruiz & Pav) have shown considerable potential as wound-healing agents. This plant has long been used in traditional medicine and contains active compounds, such as essential oils, alkaloid, saponin, tannins, and flavonoid that help accelerate healing. Reseach shows that red betel ethanol extract at 15% and 25% provide the highest wound-healing effect, achieving healing percentages of 95.83% and 98.80%, respectively, by day 15 [7]. Therefore, this study developed a stable and effective red betel extract nanoliposome ointment for topical preparation to accelerate wound healing.

Materials and methods

In silico prediction

This study employed an in-silico approach using a combination of computational software and web-based platform. The overall study design comprised several key stages: Validation of the target protein (receptor) and the compounds (ligands), molecular docking analysis, Prediction of Activity Spectra for Substances (PASS), and ADMET profiling. Bioactive compounds obtanined from *Piper crocatum* leaves were analyzed and compared with commonly used reference drugs: Celecoxib, estradiol, and Finasteride. The study focused on three-dimensional (3D) structure of these bioactive compounds, control drugs, and selected target proteins, including COX-2, ER-α (PDB) ID: IR5K), and ER-β (PDB ID: 1X7B), which are involved in the formation of pro-inflammatory cytokines. Ligand structures were sourced from the PubChem database, while protein structures were obtained from the Protein Data Bank (PDB).

A range of computational tools were employed in this study, including SWISS-MODEL, PyMOL, PyRx, Discovery Studio, PASS Online (Way2Drug), and the pkCSM web server. The workflow began with identifying bioactive compounds present in *Piper crocatum* leaves through a literature review, followed by selecting key protein associated with the phatogenesis of rheumatoid arthritis (RA). Receptor validation was perfomed using SWISS-MODEL, while ligand preparation and validation were conducted in PyRx. Protein preparation involved downloading 3D structure from the PDB in pdb format and refining them by removing native ligands and other non-essential components using PyMOL. Ligand's structures were retrieved in SDF format from PubChem and subsequently prepared for docking simulations.

Molecular docking simulations were performed using PyRx by positioning each ligand within the active sites of COX-2, Er-α, and ER-β to evaluate binding affinity and interaction characteristics. The docking results were subsequently visualized and analyzed in PyMOL and Discovery Studio, with particular emphasis on binding sites, interaction types, and binding energies. These results were then compared with those of the reference drugs. In addition, the Prediction of Activity Spectra (PA test) was performed using the PASS Online (Way2Drug) platform to estimate the potential biological activities related to rheumathoid arthritis. Finally, ADMET analysis was conducted using pkCSM to predict pharmacokinetic behavior and toxicity profiles, covering parameters such as absorption, distribution, metabolism, excretion and toxicity.

Red betel ethanol extraction

A total of 100 g of red betel leaf powder (simplisia) was collated with 70% ethanol at ratio of 1:7 (g/mL). The mixture was stirred occasionally for 48 h, and the maceration process was repeated twice. The filtrate was filtered and evaporated using a rotary evaporator at 48 °C until dry. The dried extract was then weighed and diluted to 20 mL with 70% ethanol, then washed using 30 mL (2×15 mL) of petroleum ether to remove chlorophyll, carotenoids, and lipids. Subsequently, 20 mL (2×10 mL) of absolute ethanol was added to precipitate the protein. The solution was centrified at 32,000 rpm for 20 min, after which the supernatant was re-evaporated at 48 °C, weighed, and

subjected to hydrolysis [8].

Preparation of red betel leaf extract liposomes

Liposomes were formulated using soy phosphatidylcholine (SPC) and cholesterol (CHL) at a ratio of 4:1, with 10 mL of absolute ethanol solvent and ethanol extract of red betel leaf as the active ingredient. The liposomes were prepared using the thin layer hydration method. After weighing, the components were stirred for 15 min, placed in a water bath at 60 °C for 15 min, and then stirred again for 15 min at 60 °C. The mixture was subsequently evaporated until only a layer was visible on the vial wall. Next, 3% red betel leaf extract was added, followed by hydration with 10 mL of phosphate buffer (pH 7.4). The resulting suspension was sonicated for 15 min, stirred for 1 h, and then stored in a refrigerator [9].

Preparation of red betel leaf extract liposome ointment

The ointment was prepared using the two-phase (beaker) method. For the water phase, water was heated to 80 °C; subsequently, methyl paraben, propylene glycol, and glycerin were added, and the mixture was stirred until homogeneous. For the oil phase, stearyl alcohol, stearic acid, methyl paraben, propyl paraben, and acetyl alcohol were melted at 70 °C. The two phases were then mixed and homogenized at 4,000 rpm, and Novemer® was added. After the temperature decreased to 40 - 45 °C, liposomes containing red betel extract and α-tocopherol were added and homogenized until a homogeneous ointment was obtained [10].

Table 1 The liposome red betel extract ointment formulation consists of LPC ointment at concentrations of 6%, 9%, and 12%.

Component	Control base (g)	LPC Ointment 6% (g)	LPC Ointment 9% (g)	LPC Ointment 12% (g)
Lanolin	2.97	2.79	2.70	2.61
Vaseline	16.83	15.78	15.30	14.79
BHT 1%	0.20	0.20	0.20	0.20
LPC	-	1.20	1.80	2.40
Total	20.00	20.00	20.00	20.00

Ointment characterization and evaluation:

Organoleptic evaluation

Ointment characterization and evaluation began with organoleptic assessment, involving observation of the formulation's shape and colour to determine its quality and stability. A well-prepared ointment should exhibit a homogeneous semi-solid consistency, retain the characteristic odor of the extract without developing a rancid smell, and remain free from discoloration or phase separation throughout storage. These parameters provide an initial indication of the formulation's acceptability and stability.

Further evaluations included spreadability, pH, viscosity, and physical stability test. Spreadability was measured by placing 0.5 g of ointment between two glass plates, allowing it to stand for 1 min, and then applying a 100 g load for an additional minute. The spread diameter was then recorded. Values within the ideal range of 5 - 7 cm were considered acceptable. The pH was determined using a pH meter after diluting 0.5 g of ointment in 5 mL of distilled water, with the expected pH range of 4.5 - 6.5 to match the skin pH. Viscosity was evaluated using a Brookfield viscometer to ensure consistency and stability. Additionally, physical stability testing was conducted over 28 days at room temperature to monitor changes in organoleptic properties, pH, spreadability, and viscosity.

***In vivo* wound healing assessment**

The wound-healing effectiveness study was conducted using male *Mus musculus* aged approximately 8 weeks, with an average body weight of ± 25 g. Each animal was housed individually and acclimatized for 7 days before experiment to minimize environmental stress and ansure physiological stability. For wound induction, the mice were anesthetized with ketamine (0.5 mL/kg body weight, intraperitoneally). The dorsal fur was created. The woud area was then

disinfected with a 10% iodine solution and left uncovered to allow natural healing.

Topical treatment was administered once daily until complete wound closure was achieved. A total of 20 male mice (Mus musculus) were randomly assigned to five treatment groups (n = 4 per group) to minimize bias. The experimental groups were as follows: The positive control (C+), treated with 10% povidone-iodine ointment; the negative control (C−), treated with the base ointment without the active extract; and the treatment groups receiving liposomal red betel extract (LPC) ointment at concentrations of 6% (LPC6), 9% (LPC9), and 12% (LPC12). This grouping enabled comparative evaluation of the therapeutic efficacy of the extract-based formulation against both standard treatment and untreated conditions.

Body weight of the animals was monitored every 3 - 4 days to assess general health status throughout the study. Wound-healing progress was quantitatively evaluated by measuring the wound area on days 0, 7, 10, and 14 using ImageJ, allowing calculation of mean wound area and healing rate. At the end of the treatment period, skin tissue samples from the wound site were collected for histopathological examination, focusing on re-epithelialization, granulation tissue formation, collagen deposition, inflammatory cell infiltration, and angiogenesis. Additionally, blood samples were obtained by cardiac puncture for hematological analysis to evaluate the systemic effects of the treatment on the animals' physiological condition. This study was approved by the Ethical Committee of Universitas Negeri Malang (ethical clearance No. 03.07.9/UN32.14.2.8/LT/2025).

The data are presented as mean ± standard deviation (SD) and analyzed using analysis of variance (ANOVA) to determine differences among treatment groups. When significant differences were observed ($p < 0.05$), Duncan's multiple range test (DMRT) was conducted as a post hoc analysis using SPSS version 25.

Results and discussion

Red betel leaf compounds

Based on the screening results and evaluations of drug-likeness, toxicity, ADMET, and PA values, two compounds from red betel leaf (Piper crocatum) were selected as potential wound-healing agents: Apigenin and eugenol. Eugenol was chosen as a marker compound because it is one of the predominant constituents of red betel (Piper crocatum) leaf essential oil. Previous studies have reported that the eugenol content of red betel leaf essential oil, determined by gas chromatography-mass spectrometry (GC–MS), ranges from 26.10% to 42.50% [11]. Apigenin was selected because it is a flavonoid with wound-healing potential, promoting tissue regeneration through its anti-inflammatory and regenerative activities [12]. Information regarding the canonical SMILES for each compound, along with the control drugs in the inflammatory pathway (celecoxib) and estrogen pathway (estradiol and finasteride), obtained from the PubChem database, is shown in **Table 2** [13,14].

Table 2 Red betel leaf compounds and control drugs with canonical SMILES.

No	Compounds	Canonical SMILES
1.	Apigenin	C1=CC(=CC=C1C2=CC(=O)C3=C(C=C(C=C3O2)O)O)O
2.	Eugenol	COC1=C(C=CC(=C1)CC=C)O
3.	1H-Phenalen-1-one, hydrazone	C1=CC2=C3C(=C1)C=CC(=NN)C3=CC=C2
4.	4,4'-diaminostilbene	C1=CC(=CC=C1C=CC2=CC=C(C=C2)N)N
5.	Acethydrazide,2(2-isopropyl-5-methylphenoxy)-N2-(4-carboxybenzylideno)	CC1=CC(=C(C=C1)C(C)C)OCC(=O)NN=CC2=CC=CC=C2

No	Compounds	Canonical SMILES
6.	C-(1-(4-methoxyphenyl-2-phenylethene))	COC1=CC=C(C=C1)CCC2=CC=CC=C2
7.	Euclein	CC1=CC2=C(C(=C1)O)C(=O)C=C(C2=O)C3=C(C4=C(C=C3C)C(=O)C=CC4=O)O
8.	Naphthalene	C1=CC=C2C=CC=CC2=C1
9.	Phenol, p-1-indanyl	C1CC2=CC=CC=C2C1C3=CC=C(C=C3)O
10.	Phytol	CC(C)CCCC(C)CCCC(C)CCCC(=CCO)C
11.	Vitamin E	CC1=C(C(=C(C2=C1OC(CC2)(C)CCCC(C)CCCC(C)CCCC(C)C)C)OC(=O)C)C
12.	6-Octadecenoic acid, methyl ester, (Z)	CCCCCCCCCCCC=CCCCCC(=O)OC
13.	Alpha-Humulene	CC1=CCC(C=CCC(=CCC1)C)(C)C
14.	Beta-Bisabolene	CC1=CCC(CC1)C(=C)CCC=C(C)C
15.	Gamma, terpinene	CC1=CCC(=CC1)C(C)C
16.	Methyl palmitate	CCCCCCCCCCCCCCCC(=O)OC
17.	Octadecenoic acid	CCCCCCCCCCCCCCCCC=CC(=O)O
18.	Oleic acid	CCCCCCCCC=CCCCCCCCC(=O)O
19.	Palmitic acid	CCCCCCCCCCCCCCCC(=O)O
20.	Trans-beta-farnesene	CC(=CCCC(=CCCC(=C)C=C)C)C
21.	Elemicin	COC1=CC(=CC(=C1OC)OC)CC=C
22.	Neophytadiene	CC(C)CCCC(C)CCCC(C)CCCC(=C)C=C
23.	Propionic acid	CCC(=O)O
24.	1,2,3-Propanetriol	C(C(CO)O)O
25.	2,4(1H,3H)-Pyrimidinedione	C1=CNC(=O)NC1=O
26.	4H-Pyran-4-one	C1=COC=CC1=O
27.	2-Furancarboxaldehyde	C1=COC(=C1)C=O
28.	2-Methoxy-4-vinylPhenol	COC1=C(C=CC(=C1)C=C)O

No	Compounds	Canonical SMILES
29.	2,6-Dimethyl-3-(methoxymethyl)-p-benzoquinone	CC1=CC(=O)C(=C(C1=O)C)COC
30.	1,2-Benzenedicarboxylic acid	C1=CC=C(C(=C1)C(=O)O)C(=O)O
31.	1-Methylphenazine 5-oxide	CC1=CC=CC2=[N+](C3=CC=CC=C3N=C12)[O-]
32.	9-Octadecenoic acid	CCCCCCCCC=CCCCCCCCC(=O)O
33.	Celecoxib (control)	CC1=CC=C(C=C1)C2=CC(=NN2C3=CC=C(C=C3)S(=O)(=O)N)C(F)(F)F
34.	Estradiol (control)	C[C@]12CC[C@H]3[C@H]([C@@H]1CC[C@@H]2O)CCC4=C3C=CC(=C4)O
35.	Finasteride (control)	C[C@]12CC[C@H]3[C@H]([C@@H]1CC[C@@H]2C(=O)NC(C)(C)C)CC[C@@H]4[C@@]3(C=CC(=O)N4)C

Violation and toxicity of red betel leaf compounds and control drugs

The violations of each red betel leaf compound and the control drug were obtained using the SwissADME web server. The violation values for the red betel leaf compounds and the control drug are shown in **Table 3**.

Table 3 Drug-likeness screening based on the violation of red betel leaf compounds.

Compounds	Violation			
	Lipinski	Veber	Egan	Ghose
Apigenin	0	0	0	0
Eugenol	0	0	0	0
1H-Phenalen-1-one, hydrazone	0	0	0	0
4,4’-diaminostilbene	0	0	0	0
Acethydrazide,2(2-isopropyl-5-methylphenoxy)-N2-(4-carboxybenzylideno)	0	0	0	0
C-(1-(4-methoxyphenyl-2-phenylethene))	0	0	0	0
Euclein	0	0	0	0
Naphthalene	1	0	0	2

Compounds	Violation			
	Lipinski	**Veber**	**Egan**	**Ghose**
Phenol, p-1-indanyl	0	0	0	0
Phytol	1	1	1	1
Vitamin E	1	1	1	3
6-Octadecenoic acid, methyl ester, (Z)	1	1	1	1
Alpha-Humulene	1	0	0	0
Beta-Bisabolene	1	0	0	0
Gamma, terpinene	0	0	0	1
Methyl palmitate	1	1	0	1
Octadecenoic acid	1	1	1	1
Oleic acid	1	1	1	1
Palmitic acid	1	1	0	0
Trans-beta-farnesene	1	0	0	0
Elemicin	0	0	0	0
Neophytadiene	1	1	1	1
Propionic acid	0	0	0	3
1,2,3-Propanetriol	0	0	0	4
2,4(1H,3H)-Pyrimidinedione	0	0	0	4
4H-Pyran-4-one	0	0	0	3
2-Furancarboxaldehyde	0	0	0	3
2-Methoxy-4-vinylPhenol	0	0	0	1
2,6-Dimethyl-3-(methoxymethyl)-p-benzoquinone	0	0	0	0
1,2-Benzenedicarboxylic acid	0	0	0	1

Compounds	Violation			
	Lipinski	**Veber**	**Egan**	**Ghose**
1-Methylphenazine 5-oxide	0	0	0	0
9-Octadecenoic acid	1	1	1	1
Celecoxib (control)	0	0	0	1
Estradiol (control)	0	0	0	0
Finasteride (control)	0	0	0	0

Compound violation assessment was performed according to four rules by Lipinski, Veber, Egan, and Ghose. Based on these four perspectives, it is known that a drug must have zero violations [15]. **Table 3** shows that 11 compounds in red betel leaf (Apigenin, Eugenol, 1H-Phenalen-1-one, hydrazone, 4,4'-diaminostilbene, Acethydrazide, 2(2-isopropyl-5-methylphenoxy)-N2-(4-carboxybenzylideno), C-(1-(4-methoxyphenyl-2-phenylethene)), Euclein, Phenol, p-1-indanyl, Elemicin, and 2,6-Dimethyl-3-(methoxymethyl)-p-benzoquinone, 1-Methylphenazine 5-oxide) showed zero violations. In contrast, the control drug, Celecoxib, has one violation according to Ghose criteria.

The toxicity of red betel leaf compounds and the control drug were analyzed using the Protox 3.0 web server. The results indicated the compound's active and inactive properties based on five indicators (hepatotoxicity, cardiotoxicity, immunotoxicity, mutagenicity, and cytotoxicity). The toxicities of the red betel leaf compounds and the control drug are presented in **Table 4**.

Table 4 Toxicity evaluation of red betel leaf compounds and the control drug.

No	Compounds	H	Car	I	M	Cy
1.	Apigenin	In	In	In	In	In
2.	Eugenol	In	In	In	In	In
3.	1H-Phenalen-1-one, hydrazone	Ac	Ac	In	Ac	In
4.	4,4'-diaminostilbene	In	Ac	In	Ac	In
5.	Acethydrazide,2(2-isopropyl-5-methylphenoxy)-N2-(4-carboxybenzylideno)	Ac	Ac	In	Ac	In
6.	C-(1-(4-methoxyphenyl-2-phenylethene))	Ac	In	Ac	In	In
7.	Euclein	In	In	Ac	In	In
8.	Phenol, p-1-indanyl	In	In	In	In	In

9.	Elemicin	In	Ac	In	Ac	In
10.	2,6-Dimethyl-3-(methoxymethyl)-p-benzoquinone	In	In	In	In	In
11.	1-Methylphenazine 5-oxide	In	In	In	In	In
12.	Celecoxib (control)	In	Ac	In	In	In
13.	Estradiol (control)	In	In	Ac	In	In
14.	Finasteride (control)	In	In	Ac	In	In

Note: H = Hepatotoxicity, Car = Carcinogenicity, I = Immunotoxicity, M = Mutagenicity, Cy = Cytotoxicity; In = Inactive, Ac = Active.

A good drug candidate should be inactive for these five indicators. **Table 4** shows that five compounds in red betel leaf, including Eugenol, Apigenin, Phenol, p-1-indanyl, Elemicin, 2,6-Dimethyl-3-(methoxymethyl)-p-benzoquinone, and 1-Methylphenazine 5-oxide, were inactive or non-toxic with respect to hepatotoxicity, carcinogenicity, immunotoxicity, mutagenicity, and cytotoxicity. In contrast, the control drug, Celecoxib, has been shown to exhibit cardiotoxicity, while Estradiol and Finasteride exhibit immunotoxicity.

Docking of red betel leaf compounds and control drugs

Wound healing is an acute biological process involving inflammation, proliferation, and tissue remodeling. In the early inflammatory phase, activation of cyclooxygenase-2 (COX-2) plays a critical role in prostaglandin synthesis, triggering pain, edema, and a local inflammatory response. Meanwhile, the estrogen pathway further modulates inflammation and stimulates fibroblast proliferation and re-epithelialization by activating estrogen receptor alpha (ER-α) and beta (ER-β) [16].

COX-2 was chosen as a molecular target because it plays a crucial role in the early inflammatory phase of wound healing through prostaglandin synthesis, which triggers pain, edema, and a local inflammatory response. Regulation of COX-2 activity is necessary to control inflammation and facilitate progression to the proliferation phase and optimal tissue-remodeling phase. In addition to its inflammation role, controlled COX-2 expression is also known to support cell migration, angiogenesis, and new tissue formation during wound healing [17]. Based on this mechanism, celecoxib was chosen as the control drug because it is a COX-2 receptor inhibitor widely used as a standard in anti-inflammatory pathways and molecular docking studies related to inflammation and wound healing. Celecoxib reduces tissue inflammation by selectively inhibiting COX-2-mediated synthesis of pro-inflammatory prostaglandins while having minimal effects on COX-1 activity [18].

The inflammatory pathways, estrogen receptor alpha (ER-α) and estrogen receptor beta (ER-β), were chosen as targets because estrogen plays a critical role in fibroblast proliferation, angiogenesis, collagen synthesis, re-epithelialization, and skin tissue remodeling during the wound healing process. Activation of ER-α and ER-β can accelerate wound regeneration and closure by stimulating cell proliferation and extracellular matrix formation. Based on this mechanism, estradiol was chosen as a positive control because it is a natural agonist of ER-α and ER-β, known to increase fibroblast proliferation and tissue remodeling. Meanwhile, finasteride was used as an antagonistic control because androgens have been reported to negatively affect the wound healing process.

The use of estradiol and finasteride as reference ligands was also based on previous studies investigating phytoestrogens activity on ER-α and ER-β in a molecular docking-based wound healing model [19].

The three-dimensional structures of the target proteins cyclooxygenase-2 (COX-2), estrogen receptor alpha (ER-α/1R5K), and estrogen receptor beta (ER-β/1X7B) were obtained from the Protein Data Bank (PDB) through the RCSB Protein Data Bank website. Protein preparation was performed using BIOVIA Discovery Studio 2025 by removing water molecules, ions, and native ligands bound to the proteins. The ligand structures of apigenin, eugenol, celecoxib, estradiol, and finasteride were obtained from PubChem in SDF format. Ligand preparation was performed using Open Babel in PyRx 0.8 through energy minimization with the MMFF94 force field to obtain the lowest energy conformation. All ligands were then converted to PDBQT format before molecular docking [20].

Molecular docking was performed using the CB-Dock2 web platform. The target protein structure in PDB format was uploaded to the CB-Dock2 server. A blind docking approach was employed, indicating that the binding site location was not manually determined by the researcher. Instead, the entire protein surface was explored by the system to identify the most potential binding sites before the docking process. Docking results were evaluated based on binding affinity (BA), interactions between protein amino acid residues and ligands, and binding positions. The complex with the lowest binding affinity (most negative binding energy) was selected for further analysis. Protein-ligand interaction visualization was performed using BIOVIA Discovery Studio Visualizer [21].

The binding affinity (BA) results are shown in **Table 5**. The bioactive compounds from red betel leaf have relatively low total BA values compared to control drugs in both the inflammatory and estrogen pathways. Lower BA values indicate better binding [22], as they reflect a lower and more efficient energy requirement for bond formation [23]. **Table 5** shows the Binding Affinity (BA) data from the docking of the red betel compound with the target ligand.

Table 5 Binding affinity (BA) results of the red betel compound with the target ligand.

Antiinflammation pathway			
Ligand_COX-2		**BA**	
Celecoxib (control)		–8.5	
Apigenin		–10	
Eugenol		–7.4	
Tetrahydrocurcumin		–8.6	
Estrogen pathway			
Ligand-1R5K	**BA**	**Ligand-1X7B**	**BA**
Estradiol (+ control)	–10.1	Estradiol (+ control)	–10.5
Finasteride (– control)	–7.6	Finasteride (– control)	–8.2
Apigenin	–8.7	apigenin	–9.0
Eugenol	–6.0	eugenol	–6.9
Tetrahydrocurcumin	–8.9	tetrahydrocurcumin	–6.6

The docking results, including amino acid residues involved in the interactions between red betel leaf compound and the control drug, are presented in **Table 6**. These interactions comprise hydrogen bonds and

other non-covalent interactions. This is because hydrogen bonds are stronger than other bonds [24]. The hydrogen bonds formed between the ligand and the receptor enhances the stability between the complexes. **Table 6** below summarizes the amino acid residues formed in the docking results of the red betel leaf compound with the target ligand.

Table 6 Amino acid residues in the docking results of red betel compounds with target ligands.

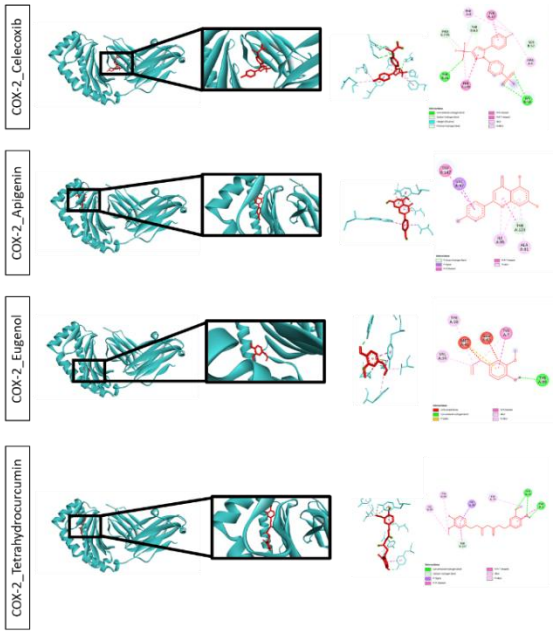
Antiinflammation Pathway				
Ligand_COX-2	**Amino acids residues**			
	Hydrogen Bond		**Others**	
Celecoxib (control)	TYR B: 26 LYS B: 58 PRO A: 235 TYR B: 63 SER B: 57		PHE A: 8 ARG A:6 PHE A: 241 TYR A:27	
Apigenin	TYR A: 123		TRP A: 147 ILE A: 95 ALA A: 81; VAL A: 97	
Eugenol	TYR A: 99		TYR A: 59 VAL A: 34 TYR A: 7; MET A:45 GLU A: 53	
Tetrahydrocurcumin	TYR A: 123 SER A: 70 TYR A: 9		ILE A: 80 TYR A: 84 TYR A: 74 ILE A: 95	
Estrogen Pathway				
Ligand	**1R5K**		**1X7B**	
	Hydrogen Bond	**Others**	**Hydrogen Bond**	**Others**
Estradiol (+ control)	GLU B: 353	PHE B: 404 ALA B: 350 MET B: 388 LEU B: 391 LEU B: 387 LEU B: 346 ILE B: 424 MET B: 421	GLU A: 305	PHE A: 356 ALA A: 302 LEU A: 343 MET A: 340 LEU A: 339 LEU A: 298 ILE A: 376 HIS A: 475 ILE A: 373
Finasteride (- control)	LEU C: 536 ASP C: 351	MET C: 421 ILE C: 424 LEU C: 525 TRP C: 383 ALA C: 350	HIS A: 498 LYS A: 471	MET B: 473
Apigenin	THR B: 347	LEU B: 346 PHE B: 404 LEU B: 525 ALA B: 350 LEU B: 387 LEU B: 391 GLU B: 353	GLU B: 305	MET B: 336 PHE B: 356 LEU B: 343 LEU B: 339 LEU B: 298 ARG B: 346
Eugenol	ARG C: 394	MET C: 357 TRP C: 360 PRO C: 324 TRP C: 393 PHE C: 445 GLU C: 353	ARG B: 346 VAL B: 280	TRP B: 312 PRO B: 277 LYS B: 401 VAL B: 338 HIS B: 279 GLU B: 305
Tetrahydrocurcumin	TYR A: 331 THR C: 347	TYR C: 537 PHE C: 404 LEU C: 525 LYS C: 529 ALA C: 350 LEU C: 346 LEU C: 387 LEU C: 391	ASN A: 470 GLU A: 474	LYS B: 471 MET B: 473 LYS A: 471

Note: Amino acid residues in bold indicate amino acid residues that are similar to the control drug.

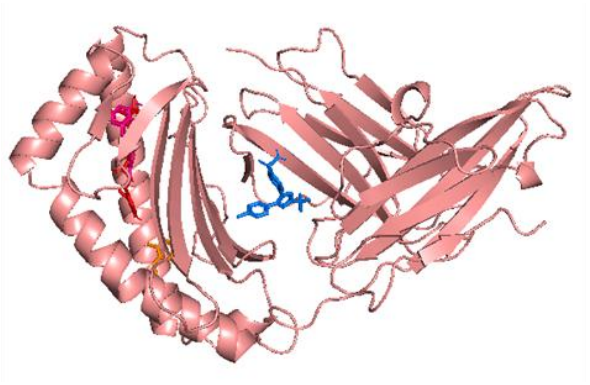
The bioactive compounds from red betel leaves share several amino acid residues, forming hydrogen bonds and other bonds with the control drug in both target pathways. The greater number of amino acid residues results in stronger ligand's bond with the target receptor or enzyme [25]. These indicate that the red betel leaf compound complex has more amino acid residues, suggesting a stronger bond compared to the control drug complex.

The docking visualization results of the red betel

leaf compound and the control drug with the COX-2 enzyme using Discovery Studio, are shown in **Figure 1**. The results obtained show two visualization models. **Figure 1(a)** visualizes the interaction of each compound, with blue represents the target enzyme and red represents the ligand. **Figure 1(b)** shows the overall docking visualization of the red betel leaf compound with the target enzyme. In this model, red represents eugenol, magenta represents apigenin, blue represents celecoxib, and green represents the target enzyme (COX-2). Although the herbal compound from red betel leaf has a different binding position than the control drug, their complexes involve a higher total number of interacting amino acid residues, as shown in **Figure 1**. The docking visualization of the red betel leaf compound and the control drug are presented below.



(a)



(b)

Figure 1 Visualization of the docking results of the red betel leaf compound and Celecoxib compound with the COX-2 enzyme. (a) Visualization of each compound; (b) Visualization of all compounds.

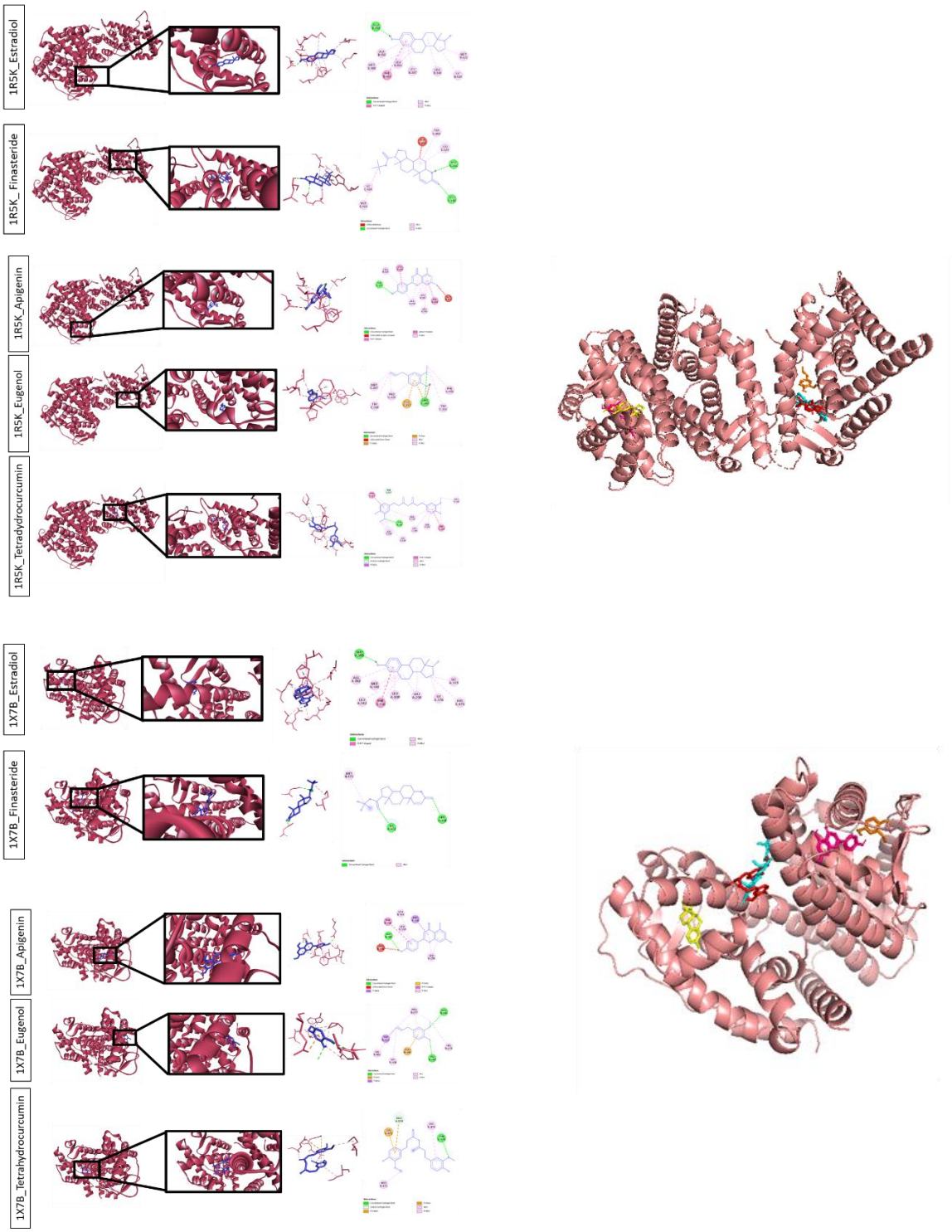


Figure 2 Visualization of the docking results of the red betel leaf compound, estradiol and finasteride, with estrogen receptor alpha (ER-α/IR5K), and beta (ER-β/1X7B) enzymes. (a) Visualization of each compound; (b) Visualization of all compounds.

The docking visualizations of the red betel leaf compounds and the control drugs with estrogen receptor alpha (ER-α/IR5K) and beta (ER-β/1X7B) enzymes, generated using Discovery Studio, are presented in **Figure 2**. Two visualization models were obtained. **Figure 2(a)** illustrates the interaction of each compound, with magenta representing the target enzyme and blue representing the ligand. **Figure 1(b)** presents the overall docking visualization of red betel leaf compounds with the target enzyme. In this model, red represents tetrahydrocurcumin, orange represents eugenol, magenta represents apigenin, yellow represents estradiol, blue represents finasteride, and pink represents target enzyme (1R5K and 1X7B). Although the red betel leaf compounds exhibited binding positions different from those of the positive control (estradiol) and negative control (finasteride), similar to the findings for the inflammatory pathway, the resulting complexes involved a greater total number of interacting amino acid residues, as shown in the figure. This multi-target approach aligns with the biological characteristics of acute wound healing, which requires rapid control of inflammation, followed by coordinated activation of tissue proliferation and remodeling. **Figure 2** shows a docking visualization of red betel leaf compounds and a control drug.

The pharmacokinetic properties of red betel leaf compounds and control drugs pharmacokinetic properties were tested using the predicting small molecule pharmacokinetic and toxicity (pkCSM) web server. The assessed parameters included absorption, distribution, metabolism, excretion, and toxicity, as shown in **Table 7** below.

Table 7 Pharmacokinetic properties of red betel leaf compounds and control drugs.

Ligand	**A**			**D**		**M**		**E**			**T**		
	Intestinal absorption (human) (% Absorbed)	**$CaCO_2$ permeability (log Papp in 10-6**	**Skin Permeability**	**Total Clearance (log**	**Total Clearance (log**	**CYP3A4 substrate**	**CYP3A4 inhibitor**	**Total Clearance (log**	**Renal OCT2 substrate**	**AMES toxicity**	**Max. tolerated dose (human) (log**	**Hepatotoxicity**	**Skin Sensitisation**
Apigenin	93.25	1.007	−2.735	0.822	−0.734	No	No	0.566	No	No	0.328	No	No
Eugenol	92.041	1.559	−2.207	0.24	0.374	No	No	0.282	No	Yes	1.024	No	Yes
Phenol, p-1-indanyl	94.115	1.538	−4.84	0.568	0.769	Yes	No	0.103	No	No	0.446	Yes	Yes
2,6-Dimethyl-3-(methoxymethyl)-p-benzoquinone	100	1.223	−6.61	−0.095	−0.13	No	No	0.68	No	No	0.873	No	Yes
1-Methylphenazine 5-oxide	98.028	1.484	−6.16	0.967	0.304	Yes	No	0.652	No	Yes	−0.002	No	No
Celecoxib (control)	93.362	1.114	−3.13	−0.969	−0.801	Yes	No	0.451	No	Yes	0.919	Yes	No

Ligand	A			D		M		E		T		
	Intestinal absorption (human) (% Absorbed)	$CaCO_2$ permeability (log Papp in 10-6	Skin Permeability	Total Clearance (log	Total Clearance (log	CYP3A4 substrate	CYP3A4 inhibitor	Total Clearance (log	Renal OCT2 substrate	AMES toxicity	Max. tolerated dose (human) (log	Hepatotoxicity	Skin Sensitisation
Estradiol (control)	94.099	1.505	−3.024	0.389	0.341	Yes	No	0.739	No	No	0.883	No	No
Finasteride (control)	93.742	1.269	−3.463	−0.185	−0.18	Yes	No	0.38	Yes	No	−1.355	Yes	No

Note: A compound is considered to have good absorption when its absorption value is >80% and moderate absorption when it is <30%. A compound is considered to have high Caco-2 permeability when its predicted value is >0.90. Compounds with a logKp value below -2.5 are generally considered to have good skin penetration. A compound is considered low when it is below 0.71 L/kg (Log VDss <-0.15) and high when it is above 2.81 L/kg (Log VDss >0.45). A compound is considered to have good blood-brain barrier penetration when its Log BB value is >0.3 and poor blood-brain barrier penetration when its Log BB value is <-1. Total Clearance <2 is considered low, and high when it is <8. MRTD ≤ 0.477 is considered low, while MRTD ≥ 0.477 is considered high.

ADMET Analysis

The pharmacokinetic analysis indicated that both the natural compounds and the reference drugs exhibited generally high intestinal absorption, with values exceeding 80%. Among them, estradiol (94.099%) and epigenin (93.25%) showed the highest absorption. In line with this, most compounds demonstrated favorable Caco-2 permeability values (>0.90 Papp in 10^{-6} cm/s). The strongest permeability across the Caco-2 model was observed in eugenol (1.559 Papp in 10^{-6} cm/s) and estradiol (1.505 Papp in 10^{-6} cm/s). Skin permeability (logKp) values among the natural compounds were relatively comparable, with apigenin and eugenol showing values of −2.735 and −2.207, respectively. The control drugs showed similar trend, including finasteride (−3.463), celecoxib (−3.13), and estradiol (−3.024). since more negative logKp value indicate better transdermal penetration, most compounds from red betel leaves demonstrated forable skin permeability, although the control drugs showed slightly better performance in relation to PA-assosiated penetration.

Intestinal absorbtion plays a key role in determining systemic drug availability and ultimately affects therapeutic outcomes. Compounds are generally considered acceptable when intestinal absobption reaches at least 30% and Caco-2 permeability exceed 0.9 [26]. Similarly, skin permeability, expressed as logKp (cm/h), reflect the efficiency of transdermal delivery, with values below −2.5 generally indicating good penetration [27]. In terms of distribution, apigenin exhibited the highest volume of distribution at steady state (VDss) among the natural compound (0.822 L/kg), while celecoxib showed the highest value among the control drugs (0.969 L/kg). Higher VDss values indicates more extensive distribution into body tissue. In general, VDss is considered low when greater than −0.15 L/kg and high when exceeding 0.45 L/kg. Regarding blood-brain barrier permeability, eugenol (0.374 log BB) and estradiol (0.389 log BB) showed the highest values, suggesting a stronger potential for central nrvous system distribution [26].

Metabolic profiling revealed that apigenin and eugenol are neither substrates nor inhibitors of CYP3A4, Indicating that they are unlikely to be metabolized through this pathway or interfere with its activity [28]. All control drugs were classified as CYP3A4 substrates but not inhibitors. In terms of excretion, epigenin (0.566 log mL/min/kg) and estradiol (0.739 log mL/kg) demonstrated the highest total clearance values, suggesting relatively rapid elimination, wich is generally considered beneficial [29]. None of the evaluated red betel leaf compounds or control drugs (celecoxib and estradiol) were substrates of the renal Organic Cation Transporter 2 (OCT2); only finasteride indicated a minimal role of OCT2-mediated renal clearance [28]. Toxicity predictions further

indicated that apigenin, estradiol, and finasteride, were non-mutagenic based on the AMES test. Eugenol showed the highest maximum tolerated dose (1.024), suggesting better tolerance at higher exposure levels compared to other compounds and reference drugs. However, hepatotoxicity assessment revealed that all compounds and control drugs were non-hepatotoxic, with the exception of eugenol [29].

Potency Activity (PA) of red betel leaf compounds and the control drug

The Potency Activity (PA) analysis indicated that the bioactive compounds from red betel leaves demonstrated good performance to support wound healing through biological mechanisms. Higher PA value indicates better compound potential. The PA values of the red betel leaf compound and the control drug sre shown in **Table 8**.

Table 8 Potency Activity (PA) of red betel leaf compound and the control drug.

Ligand	PA Value				
	Antiinflammatory	**Antioxidant**	**Angiogenesis stimulant**	**MMP9 expression inhibitor**	**Skin irritation, inactive**
Apigenin	644	732	555	780	171
Eugenol	491	463	326	797	611
Tetrahydrocurcumin	598	473	282	876	178
Celecoxib (control)	663	-	-	-	-
Estradiol (control)	427	288	-	646	-
Finasteride (control)	-	-	-	-	-

Based on **Table 8**, apigenin and the control drug celecoxib showed the highest PA values, at 644and 663, respectively. Anti-inflmammatory activity plays a key role in suppressing inflammatory mediators by inhibiting cyclooxygenase (COX), lipoxygenase (LOX), and phospholipase A2, threreby reducing inflammation in the early phase of wound healing [30]. Additionally, apigenin exhibited the highest antioxidant PA (732), whereas celecoxib and finasteride showed no antioxidant PA activity. Antioxidant activity reactive oxygen species (ROS), reducing oxidative stress, and protecting cellular integrity during tissue repair [31].

During the proliferative phase, the stimulation of angiogenesis and fibroblast activity is crucial for effective wound healing [32]. Apigenin demonstrated the highest angiogenesis PA value (555), while control drugs showed no such activity. Furthermore, strong Matrix Metalloproteinase-9 (MMP-9) inhibitory activity in eugenol and apigenin supports extracellular matrix stability and enhances tissue remodeling [33]. Regarding safety, eugenol showed lower skin irritation potential, making it more suitable for topical use. Overall, the combination of anti-inflammatory, antioxidant, angiogenic, and MMP-9-inhibitory activities suggests that these compounds may act synergistically throughout the wound-healing process.

Organoleptic observations

Preliminary results show that red betel liposomes have a PDI of 0.4, Z-average of 122.38 nm, zeta potential of –28.8 mV, and an Encapsulation Efficiency (EE) value of 99.9%. Based on SEM results, red betel liposomes have a size of 139 nm. The formulation results indicated that all preparations (including controls) have a semi-solid texture, consistent with the characteristics of topical preparations made from lanolin

and petroleum jelly (**Table 9**). Upon application, the formulations produced a moisturizing effect on the skin, indicating good emollient and occlusive properties. These characteristics help maintain skin hydration by reducing transepidermal water loss (**Figure 3**). This result aligns with the properties of lanolin and petroleum jelly, which moisturize and protect the skin without causing excessive stickiness if the formula is stable. Based on the literature, lanolin can moisturize, soothe, and repair the skin's protective layer, making it a common ingredient in ointments for dry or irritated skin [34].

Table 9 Results of organoleptic testing of red betel extract ointment formula.

Formula	Appearance	Sensation After Application (Sticky /Wet / No)	Homogenites
Control	Semi solid	Humid	Homogeneous
LPC6	Semi solid	Humid	Homogeneous
LPC9	Semi solid	Humid	Homogeneous
LPC12	Semi solid	Humid	Homogeneous

Note: Control; base ointment; LPC6: liposome extract ointment with wider measures of 6%; LPC9: liposome extract ointment with wider measures of 9%; LPC12: Liposome extract ointment to a wider extent of 12%.

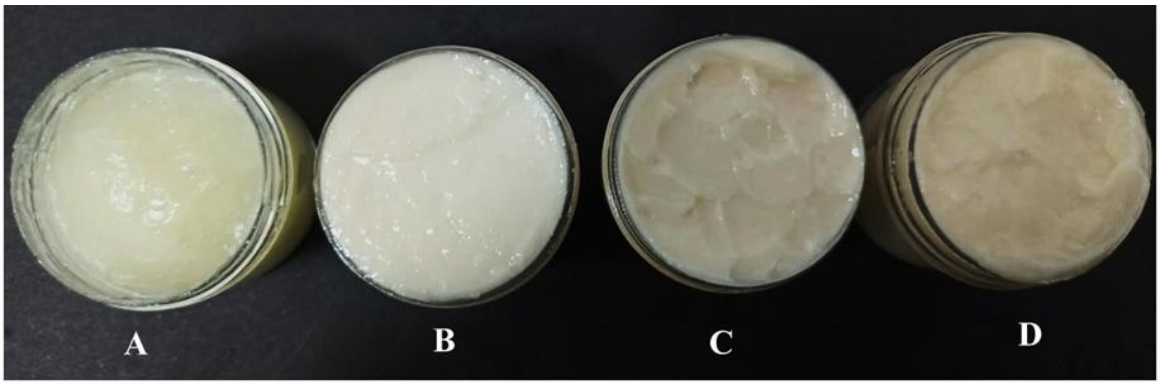


Figure 3 Red betel extract ointment formula. (Control; ointment base; LPC6: Liposomal extract ointment with wider measures of 6%; LPC9: Liposomal extract ointment with wider measures of 9%; LPC12: Liposomal extract ointment to a wider extent of 12%.

Liposomes have proven to be an effective delivery system for natural products due to their various advantages. This system can reduce side effects, improve drug targeting, and manage to avoid degradation in the gastrointestinal tract and liver metabolism. The main advantage of liposomes lies in their ability to protect active compounds while increasing their stability. Application to transdermal preparations, liposomes play an important role in increasing skin penetration, thereby improving therapeutic effect. In addition, this system enables sustained therapy through a controlled release mechanism. These advantages make liposomes an ideal choice for both transdermal and systemic application of natural product [35].

Stability test

The results of the pH test show that all red betel extract ointment has pH ranging from 4.8 to 6.0, which are within the physiological pH range of the skin (**Figure 4**). After 28 days of storage at 4, 25, and 40 °C, there was a slight but not statistically significant decrease in pH ($p > 0.05$), indicating formulation stability under different temperature conditions. Difference between formulation, indicated by different letters, suggest compositional variations that affect pH values; however, all values remained the safe range for topical application. The graph shows that the pH of all formulas was relatively stable from 0 to day 28 (pH range: ±5.0). There is no drastic decline indicating chemical degradation or system instability. This pH stability is important for skin comfort and the

effectiveness of the active ingredients. Stability studies of lanolin-petroleum jelly ointment bases showed that pH tends to be stable during storage. Previous studies have also reported that such ointment bases may experience discoloration and the presence of supernatants after long storage, but no change in smell.

Dispersion and increased viscosity may also occur but remain within reasonable limits for semi-solid preparations [36]. Lanolin is scientifically proven to have a moisturizing, anti-inflammatory, and improving skin barrier effects, including in animal models with dermatitis [34]. Petroleum jelly functions as an occlusive agent, retaining moisture by preventing water evaporation from the skin surface. The use of liposomes can increase the penetration of active ingredients while strengthening the skin barrier, especially if lipids similar to stratum corneum or lanolin are used [37].

Red betel leaf extract contains a variety of active compounds, especially flavonoids (such as quercetin and brazilin), terpenoids, tannins, saponins, and eugenol. These compounds have been scientifically proven to have strong anti-inflammatory activity [38]. The main anti-inflammatory mechanisms include the decreased pro-inflammatory cytokines, inhibition of COX pathways and lipooxygenase, which play a role in the formation of inflammatory mediators such as prostaglandins and leukotriene, and regulation of transcription factor NF-κB, thereby lowering the secretion of pro-inflammatory cytokines and inhibiting the migration of leukocytes to inflammatory areas [37,38].

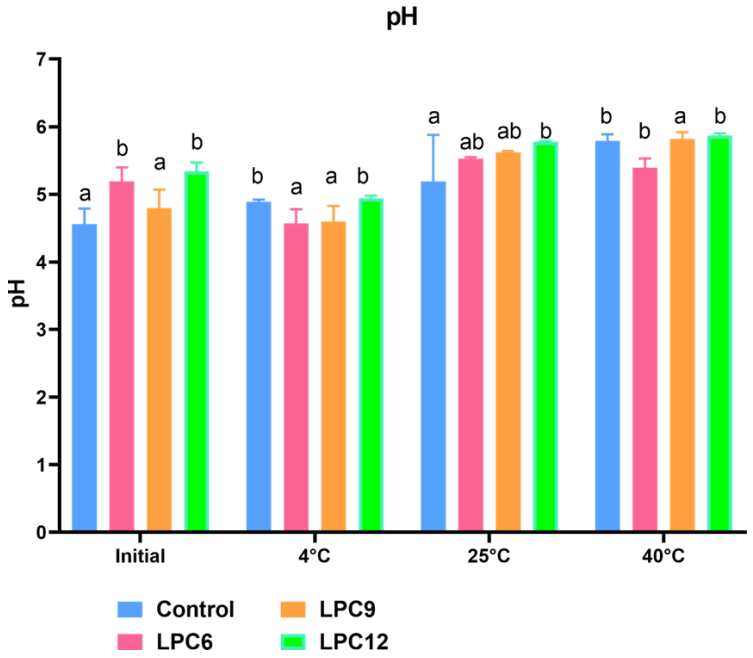


Figure 4 The pH test results of the red betel extract ointment formula before and after storage for 28 days at a temperature of 4, 25, and 40 °C. (Remarks: Control; ointment base; LPC6: Liposome ointment of 6% red betel extract; LPC9: 9% red betel extract liposome ointment; LPC12: 12% red betel extract liposome ointment. The data were presented in the form of mean ± standard deviation (SD) Statistical analysis used one-way ANOVA followed by the Duncan Multiple Range Test (DMRT ($p < 0.05$).

A pH of around 5 is considered optimal for transdermal ointment formulations because it is close to the skin's natural pH, which ranges from 4 to 6, thus minimizing irritation and maintaining skin barrier integrity [30]. This pH also supports the stability and solubility of the drug in the ointment, which is essential for effective dermal drug penetration. Research shows that at a pH of around 5, particularly for weakly basic drug, increased ionization enhances drug solubility, thereby increasing flux and skin permeability, especially in modified skin such as after microneedle (MN). Higher drug flux enables effective drug concentration to be achieved with smaller patch size or doses [40].

Dispersion test

Statistically, the grafh showed no significant difference ($p > 0.05$) in dispersion values between the ointment base control and the *Piper crocatum* extract liposomes ointment throughout the observation period. The graph shows the result of the dispersion test of several ointment formulas containing red betel extract in the form of liposomes with various concentrations, as well as controls without extract (**Figure 5**). The dispersion test showed that the ointment was able to spread evenly over the glass surface. A larger spread indicates faster distribution, even with minimal contact between the drug and the surface [41]. The dispersion of the ointment is affected by the amount of base used in each formulation. Higher amounts of petroleum jelly increase the spreadability, allowing the ointment to spread more widely. In contrast, lower amounts of petroleum jelly increase ointment viscosity, thereby limiting its spread [42]. The dispersion result of the control in this study was 3 cm, which remains in the acceptable range (3 - 5 cm). these findings align with previous studies reporting that preparation with a spreadability of 3.2 and 3.7 cm were considered eligible [43].

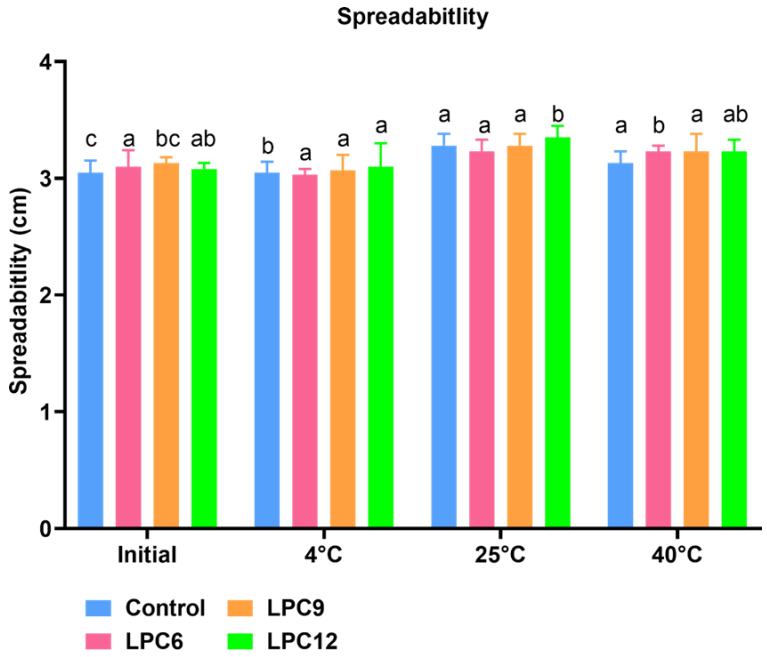


Figure 5 The results of the dispersion test of the red betel extract ointment formula before and after storage for 28 days at a temperature of 4, 25, and 40 °C. (Control; ointment base; LPC6: Liposome ointment of 6% red betel extract; LPC9: 9% red betel extract liposome ointment; LPC12: 12% red betel extract liposome ointment. The data were presented in the form of mean ± standard deviation (SD) Statistical analysis used one-way ANOVA followed by the Duncan Multiple Range Test (DMRT ($p < 0.05$).

Color evaluation

The color test data showed significant changes (**Table 10**) in color parameters between the controls and the LPC6, LPC9, and LPC12 formulas. The brightness gradually increases from control (54.00) to LPC12 (75.70), indicating that the LPC formula produces a brighter appearance. For the parameter representing the red-green color axis, values shifted from negative values at the control and LPC6 (−0.65 and −2.90) to positive in LPC12 (0.70), indicating a transition from a slightly greenish tone to a reddish tone. For the parameter representing yellow color intensity, there was a significant increase from control (9.45) to LPC12 (17.25), indicating a stronger yellow coloration in the LPC treatment. Overall, the LPC formulation produced a brighter, and a more yellow appearance, with a shift from green to red, indicating a clear and measurable color change compared to controls. The L* value indicates color brightness, ranging from black (L* = 0) to white (L* = 100). The value a* describes colors in the range from green (negative value) to red (positive value), while value b* indicates color from blue

(negative value) to yellow (positive value) $L*a*b*L*a*b*$ [44]. A negative a* value in the sample indicates a green color tendency affected by the extract color, while a positive b* value indicates a yellow tendency, likely due to the yellow wax or oil used. Samples were generally light in color, indicated by a high L* value [45,46]. The differences between the formulas were also statistically significant, suggesting that increasing LPC dose had a different effect on the sample color. The ointment preparation should not have a rancid smell, have a soft texture, and have a distinctive smell and color of the extract [47].

Table 10 Color test results of red betel extract ointment.

Formula	L	a*	b*
Control	54.00 ± 1.96^{a}	-0.65 ± 0.12^{a}	9.45 ± 0.40^{a}
LPC6	70.85 ± 1.21^{b}	-2.90 ± 0.06^{b}	15.45 ± 0.64^{b}
LPC9	73.75 ± 0.40^{c}	-0.10 ± 0.12^{c}	16.45 ± 0.17^{c}
LPC12	75.70 ± 0.35^{d}	0.70 ± 0.06^{d}	17.25 ± 0.17^{d}

Note: Control; ointment base; LPC6: Liposome ointment of 6% red betel extract; LPC9: 9% red betel extract liposome ointment; LPC12:12% red betel extract liposome ointment. Data were presented in the form of mean ± standard deviation (SD) Statistical analysis using one-way ANOVA followed by the Duncan Multiple Range Test (DMRT ($p < 0.05$).

Viscosity of red betel liposome ointment

The results of the torsion and viscosity tests showed that the addition of red betel extract liposomes to the paraffin-lanolin base consistently affected the rheological properties of the preparation (**Table 11**). The highest torque and viscosity values were recorded in SF3 (9% liposome) (34.87 ± 0.42 cP; 69,733.33 ± 837.99 cP), while SF2 (6% liposome) showed the lowest values (29.93 ± 0.82 cP; 59,866.67 ± 1,635.71 cP). The increased viscosity at 9% liposomes is likely due to interaction between liposomal phospholipids and the base lipid matrix (paraffin/lanolin), which strengthens the continuity of the organic phase and forms a denser lamellar/internal tissue structure, thereby increasing flow resistance. Previous studies have reported that the incorporation of lipid systems (liposomes/lipid particles) into topical vehiculum generally alters rheological parameters and can increase viscosity when the particles are distributed homogeneously and interact with the continuous phase [48]. In addition, the role lanolin and paraffin as components of semisolid vehiculum in increasing viscosity and altering flow behavior has been documented; variation in petroleum/lanolin composition affects base viscosity and response to the addition of the active ingredients [49].

Lanolin is a semi-solid material rich in complex ester and fatty alcohols, which can interact with the hydrocarbon chain of petroleum jelly through the van der Waals forces, forming a tigher internal network. These interactions increase resistance to deformation, resulting in higher torque and viscosity [50]. The observed viscosity decrease in SFA (12% liposome) (32.43 ± 0.63 cP ± 1.177.57 cP) can be explained by saturation effect and the possible formation of liposome aggregates or distribution heterogeneity at higher concentration, which disrupt matrix continuity and slightly reduce floe resistance, beavior that has also been reported in studies evaluating at the effect of emulsion liposomal or submicron concentration on rheological properties of topical formulation [51]. Based on these results and supporting literature, SF3 (9% liposome) becomes the most optimal composition candidate in terms of rheological properties, as it offers high viscosity that favour physical stability without reaching an aggregation level that reduces the homogeneity of the preparation. This balance is important for storage stability, active ingredient release, and sensory characteristics during topical application [48].

Table 11 Viscosity and torque percentage test result.

Treatment	Torque (%) (Mean ± SD)	Viscosity (CP) (Mean ± SD)
Control	31.93 ± 0.54[b]	63,866.67 ± 1,087.30[b]
LPC6	29.93 ± 0.82[a]	59,866.67 ± 1,635.71[a]
LPC9	34.87 ± 0.42[c]	69,733.33 ± 837.99[c]
LPC12	32.43 ± 0.63[b]	64,800.00 ± 1,177.57[b]

Note: Control; ointment base; LPC6: Liposome ointment of 6% red betel extract; LPC9: 9% red betel extract liposome ointment; LPC12: 12% red betel extract liposome ointment. Data were analysis used one-way ANOVA followed by the Duncan Multiple Range Test (DMRT ($p < 0.05$).

Weight loss during wound healing

More stble weight change in the LPC9 and LPC12 group indicated better physiological conditions during the healing process. A significant increase in body weight ($p < 0.05$) compared to negative controls indicated more stable metabolic condition and improved energy use efficiency in the wound healing phase. In contact, the negative control group experience weight loss, likely due to infmmatory stress and metabolic imbalaces associated with delayed healing (**Figure 6**). Thus, the weight gain observed in the treatment group reflects better nutritional status and is also closely related to the body's physiological effectiveness in supporting tissue regeneration.

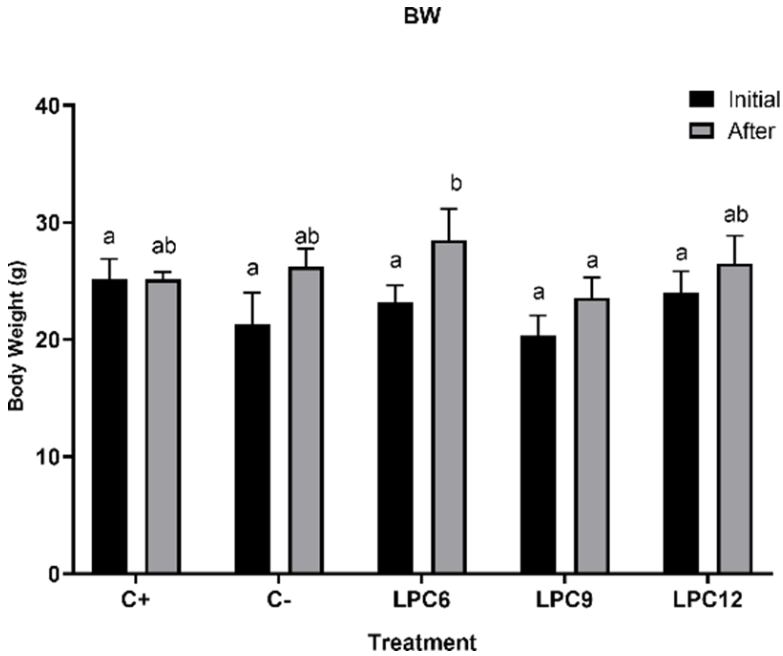


Figure 6 The weight of mice showed after injury and the administration of red betel liposome ointment. (C+: 10% iodine; C-: Ointment base; LPC6: Liposome ointment of 6% red betel extract; LPC9: 9% red betel extract liposome ointment; LPC12: 12% red betel extract liposome ointment. Data were presented in the form of mean ± standard deviation (SD) Statistical analysis used one-way ANOVA followed by the Duncan Multiple Range Test (DMRT ($p < 0.05$).

Physiologically, the limited weight gain in the LPC6 group is likely due to moderate antioxidant and anti-inflammatory activity, resulting in a suboptimal metabolic balance. However, an adequate early wound healing response suggests that this dose is sufficient to stimulate tissue regeneration without causing excessive metabolic stress. This consistency in body weight aligns with the findings that normal mice tend to maintain their weight during wound healing. Another study also reported no significant difference in injured mice. A temporary decrease in feed intake was observed for 24 h after injury, but there was no significant difference between sedentary and exercised mice in the wound healing model [52]. Wound healing increases the need

for calories and protein; nutritional deficiencies (either due to low intake or poor diet quality in obesity) hinder cell regeneration, immune function, and collagen formation [53,54].

The activity of liposome ointment in wound healing

The graph shows the percentage of wound contractions in each treatment group during the observation period. From day 3 to day 14, all groups experienced an increase in wound contractions, albeit at different speeds. The LPC6 group showed faster wound shrinkage in the early phase (day 3), indicating a good early regenerative response to treatment. By day 7, the LPC9 and LPC12 groups showed a higher increase in wound contraction compared to the negative control, with a significant difference ($p < 0.05$), indicating the effectiveness of the formulation in accelerating the proliferation phase. From days 10 to 14, the LPC9 and LPC12 groups achieved the highest rate of wound contraction close to positive control, indicating a near-perfect wound closure (**Figure 7**).

The trend of accelerating wound contraction in the LPC9 and LPC12 groups was followed by a decrease in exudate and the formation of better granulation tissue from day 7. This effect is likely attributable to bioactive compounds in LPC formulations, such as flavonoids, phenolics, and alkaloids, which have antioxidant and anti-inflammatory properties. This mechanism can reduce oxidative stress, suppress NF-κB activation, and stimulate fibroblast proliferation and collagen synthesis, thereby accelerating epithelialization and tissue remodeling. Overall, these results suggest that the concentrations of LPC9 and LPC12 have superior therapeutic potential in supporting wound healing compared to both the low-dose and negative control groups (**Figure 8 and 9**).

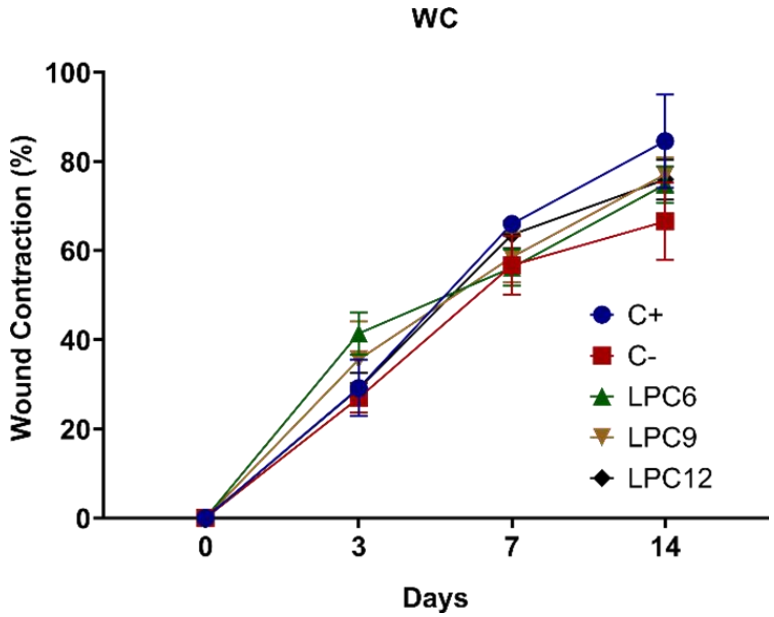


Figure 7 Wound contraction on the 3rd, 7th, and 14th day of treatment and after the administration of red betel liposome ointment. (C+: 10% iodine; C-: Ointment base; LPC6: Liposome ointment of 6% red betel extract; LPC9: 9% red betel extract liposome ointment; LPC12: 12% red betel extract liposome ointment.) Data were presented in the form of mean ± standard deviation (SD) Statistical analysis used one-way ANOVA followed by the Duncan Multiple Range Test (DMRT ($p < 0.05$).

Wound contraction is the process of shrinking the unhealed wound area during healing. Faster wound narrows indicate more effective applied treatment. This process occurs due to an increase in fibroblast cells, which contribute to new tissue formation. Some fibroblasts will turn into myofibroblasts, cells that are able to contract and pull the edges of the wound closer together. As a result, the formation of a new layer of skin (epithelialization) occurs more rapidly, so the wound heals faster [55]. This phase, known as proliferation

phase, usually begins on the 3rd day after the wound and lasts about 2 weeks. At this stage, fibroblasts move to the wound area and form a new collagen-like extracellular matrix to replace the temporary tissues of fibrin and fibronectin [56]. Higher wound contraction value indicates faster wound closure and healing, likely due to antimicrobial, anti-inflammatory, and antioxidant effects of the treatment. Contraction reduces the wound area, thereby decreasing the amount of new tissue (ECM) needed. In addition, contractions facilitate the formation of new layers of skin because skin cells do not need to move too far to close the wound [57].

On day 3, the LPC6 group showed faster wound narrowing than the other groups, indicating a good initial response to treatment. By day 7, the negative control group still showed a larger wound area, while the LPC12 group showed a healing rate equivalent to the positive control. By day 14, all treatment groups showed near-perfect wound closure, with significantly smaller wound area compared to the negative control ($p < 0.05$).

The effectiveness of the treatment in accelerating tissue regeneration was supported by increased expression of α-SMA, SOD1, and E-cadherin, as well as a decrease in p53, which plays a role in cellular stress. Bioactive compounds such as phenolics, flavonoids, saponins, alkaloids, tannins, and steroids play a synergistic role in balancing the inflammatory response and antioxidant activity [58,59]. The anti-inflammatory activity of *Piper crocatum* has also been proven in post-excision and inflammatory and wound models, where the extract reduces IL-10 and TGF-β1 levels while increasing VEGF, thereby accelerating angiogenesis and wound healing. Flavonoids play an important role by suppressing the inflammatory pathways, including NF-κB and JNK, activating the Nrf2/ARE pathway, and modulating TGF-β and PI3K/Akt signaling, thereby accelerating collagen deposition and fibroblast proliferation. Flavonoids activate Nrf2/ARE, increase antioxidant enzymes (SOD, GSH-Px, heme oxygenase, etc.), and reduce ROS, which is important in chronic wounds and diabetes [60]. In addition, flavonoids and polyphenols suppress the formation of ROS and RNS by inhibiting the enzymes COX, LOX, and phospholipase A_2, thereby reducing the production of inflammatory mediators and accelerating wound healing. Nrf2 activation counteracts NF-κB activity, as Nrf2 controls reparative inflammation and prevents excessive ROS accumulation [61]. Flavonoids suppress the activation of NF-κB and JNK, thereby reducing the expression of pro-inflammatory cytokines (TNF-α, IL-1β, IL-6), PGE_2, LTB_4, and iNOS/COX-2/LOX enzymes [62,63].

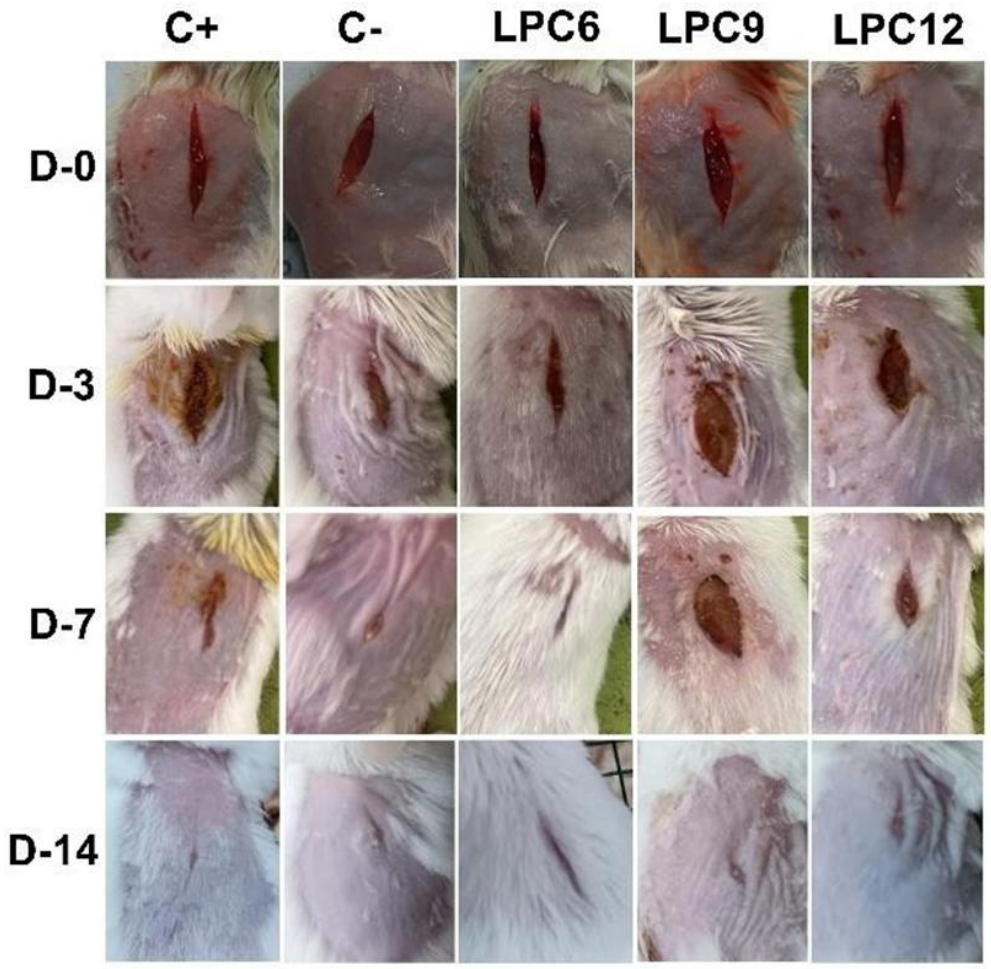


Figure 8 Photos of macroscopic observations of cut wounds on days 0, 3, 7, and 14. Mice received a topical treatment using *Piper crocatum* extract liposome ointment. (C+: 10% iodine; C-: Ointment base; LPC6: Liposome ointment of 6% red betel extract; LPC9: 9% red betel extract liposome ointment; and LPC12: 12% red betel extract liposome ointment.).

In this study, the results of re-epithelialization in the C+ group showed an average value of 381.82 ± 73.66, which was lower than the negative control (C–) of 435.38 ± 0.57, indicating that C+ treatment increase epithelial growth compared to negative conditions. The LPC6, LPC9, and LPC12 treatment group had lower re-epithelialization values compared to controls; however, LPC9 and LPC12 showed improvement that was close to positive control. Regarding wound length, the negative control (C–) showed the highest values of 562.19 ± 48.33, while LPC9 and LPC12 gave better results with marked lower values of 203.82 ± 8.22 and 109.22 ± 13.11, respectively, indicating accelerated wound healing. The highest angiogenesis parameters were observed in the LPC12 group (46.00 ± 1.41), followed by C+ and LPC9, which also showed a significant improvement compared to the negative controls. This indicates that LPC12 effectively stimulates the formation of new blood vessels, which is important in wound healing. Fibrous thicknesses, reflecting scar tissue formation, was highest in negative controls (239.73 ± 22.60), while LPC9 and C+ showed the lowest thickness, indicating better healing quality with minimal scar tissue formation (**Figure 10**). Overall, LPC9 and LPC12 treatment positively accelerated wound healing by increasing angiogenesis, reducing wound length, and controlling scar tissue formation compared to the control group. This analysis shows that LPC9 and LPC12 treatment have the potential to be an effective therapy in accelerating the process of wound tissue regeneration.

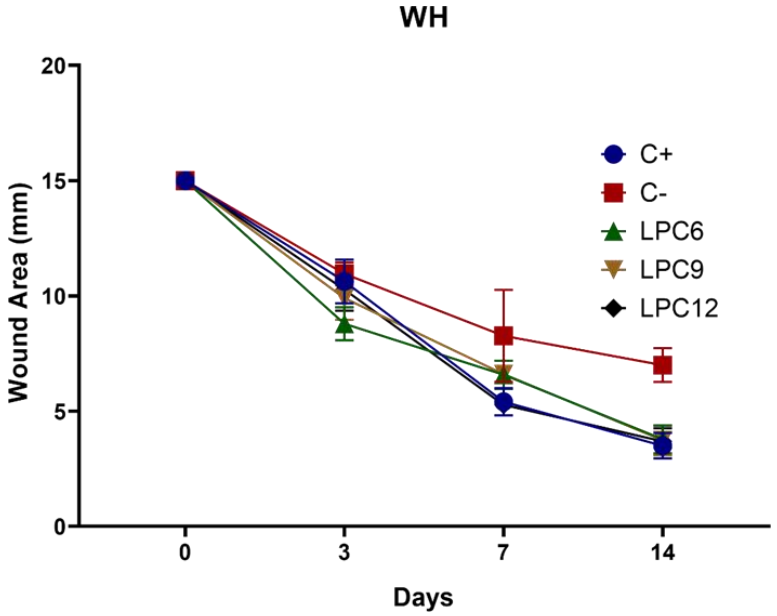


Figure 9 Wound contraction on the 3rd, 7th, and 14th day of treatment and after the administration of red betel liposome ointment. (C+: 10% iodine; C-: Ointment base; LPC6: Liposome ointment of 6% red betel extract; LPC9: 9% red betel extract liposome ointment; LPC12: 12% red betel extract liposome ointment; Data were presented in the form of mean ± standard deviation (SD) Statistical analysis used one-way ANOVA followed by the Duncan Multiple Range Test (DMRT ($p < 0.05$).

Red betel liposome ointment (LPC) has significant anti-inflammatory activity. Research shows that red betel leaf extract can induce macrophage phagocytosis activity without increasing nitric oxide (NO) production excessively, which is characteristic of acute inflammation [64]. The anti-inflammatory mechanism of LPC involves inhibition of inflammatory mediators and regulation of local immune responses in the wound area through bioactive compounds such as flavonoids, terpenoids, and phenols contained in red betel extract [65]. Liposome technology, as a drug delivery system, strengthens the effectiveness of active ingredients by increasing their penetration and stability in tissues [66].

The active compounds in red betel inhibit signaling pathways of pro-inflammatory cytokines such as TNF-αand IL-6, while increasing the expression of growth factors that support cell proliferation and the formation of new blood vessels [67]. This anti-inflammtory activity accelerates wound healing by reducing excessive inflammatory reactions that can inhibit tissue regeneration [68,69].

In the context of angiogenesis, LPC12 specifically stimulates the formation of new blood vessels, an important process in wound healing as it provides oxygen and nutrients to regenerating tissue. Growth factors such as vascular endothelial growth factor (VEGF), fibroblast growth factor (FGF), and transforming growth factor-beta (TGF-β), produced by endothelial cells and macrophages in the wound area, play a key role in cell migration, endothelial proliferation, and the formation of granulated tissue. This process of angiogenesis accelerates the removal of metabolic waste products and support optimal tissue repair [70]. Wound healing involves coordinated molecular and celluler mechanisms. In the early stages, hemostasis and keratinocyte activation occur along with inflammatory cells. The next stage involves the proliferation and migration of keratinocytes, fibroblast proliferase, matrix deposition, and angiogenesis. In the final stage, extracellular matrix (ECM) remodeling occurs, resulting in the formation of scar tissue and the restoration of the barriers. This process occurs in a spatiotemporally regulated manner and is tightly controlled by different cell types that secrete growth factors, cytokines, and chemokines to achieve closure and tissue restoration [71].

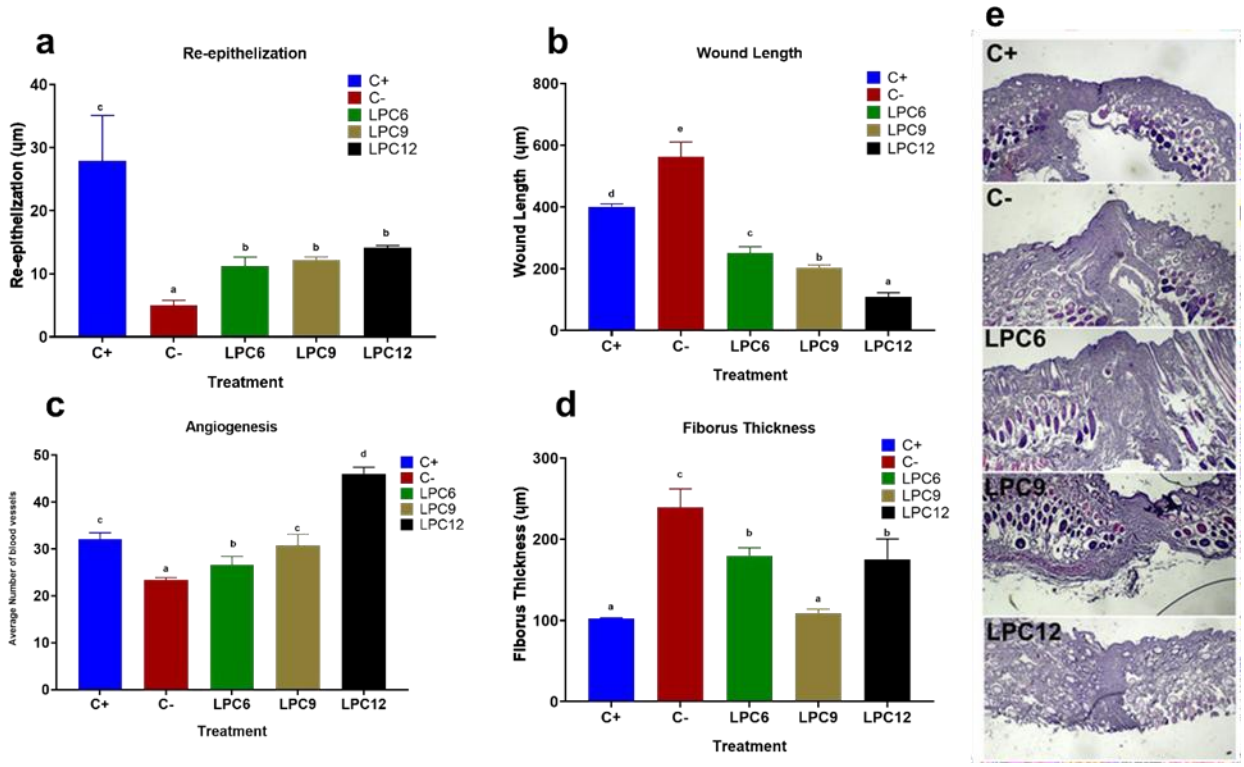


Figure 10 Skin tissue regeneration after red betel extract liposome ointment treatment based on histological parameters including (a) reepithelialization, (b) wound length, (c) epidermal thickness, (d) dermis thickness, and (e) histological picture of the skin with hematoxilin-eosin (HE) staining at 10x magnification. (C+: 10% iodine; C-: Ointment base; LPC6: liposome ointment of 6% red betel extract; LPC9: 9% red betel extract liposome ointment; and LPC12: 12% red betel extract liposome ointment.) The data were presented in the form of mean ± standard deviation (SD) Statistical analysis used one-way ANOVA followed by the Duncan Multiple Range Test (DMRT ($p < 0.05$)).

In addition to angiogenesis, LPC also controls the formation of scar tissue. Low fibrous thickness in the LPC9 and C+ groups indicate improved wound healing quality with minimal scar tissue formation, which is important for maintaining tissue function and aesthetics after wound healing. Overall, the evidence supports that red betel liposomes are effective anti-inflammatory and wound-healing agents. LPC accelerates tissue regeneration through inflammatory modulation, stimulates angiogenesis, and balanced control of fibrosis, making it a promising natural therapeutic alternative for wound treatment. Thus, red betel liposome ointment serves as an anti-inflammatory and promotes tissue regeneration, making it a potential therapeutic alternative for wound care with minimal side effects.

Blood profile

Wound healing in mice treated with red betel extract liposome ointment showed a significant effect on hematological parameters that favored the tissue regeneration process (**Table 12**). The LPC9 group showed the highest number of leukocytes at 7.93 ± 0.48 $\times 10^3/\mu L$, indicating an optimal initial inflammatory response to clear debris and microorganisms, thereby accelerating the inflammatory phase that is important for healing. The LPC12 group had the highest erythrocytes count (10.41 ± 0.00 $\times 10^6/\mu L$) and hemoglobin (12.78 ± 0.43 g/dL), which contribute to increased oxygen delivery to wound tissues, supporting metabolism and collagen synthesis. The hematocrit in LPC12 was also relatively high (38.80 ± 2.55%), indicating optimal blood volume to support tissue regeneration.

Table 12 Results of blood profile measurement of mice of cut-off wound models after the administration of liposome ointment treatment.

Parameter	C+	C−	LPC6	LPC9	LPC12
Leukocytes (×10³/μL)	5.93 ± 1.14^{ab}	6.07 ± 1.01^{ab}	4.54 ± 0.34^{a}	7.93 ± 0.48^{b}	5.29 ± 2.44^{a}
Erythrocytes (×10⁶/μL)	8.45 ± 0.18^{a}	8.05 ± 0.66^{a}	8.24 ± 0.47^{a}	8.50 ± 0.46^{a}	10.41 ± 0.00^{b}
Hemoglobin (g/dL)	11.35 ± 0.64^{a}	12.10 ± 0.43^{ab}	12.78 ± 0.43^{b}	11.80 ± 0.77^{b}	11.60 ± 0.00^{a}
Hematocrit (%)	35.73 ± 2.41^{ab}	36.21 ± 0.14^{ab}	33.69 ± 1.29^{a}	35.77 ± 2.07^{ab}	38.80 ± 2.55^{b}
Platelets (×10³/μL)	1,127.67 ± 76.84^{c}	2,091.11 ± 224.98^{a}	1,102.67 ± 104.15^{a}	1,456.67 ± 112.67^{b}	1,210.00 ± 0.00^{a}
MCV (fL)	43.33 ± 1.25^{ab}	43.33 ± 1.25^{ab}	47.33 ± 3.40^{a}	42.33 ± 0.47^{b}	46.63 ± 4.31^{b}
MCH (pg)	14.53 ± 0.62^{a}	14.25 ± 1.89^{a}	17.67 ± 2.67^{b}	13.43 ± 0.19^{a}	14.07 ± 1.08^{a}
RDW (%)	19.23 ± 0.50^{a}	20.50 ± 2.24^{ab}	18.13 ± 0.93^{a}	22.17 ± 0.24^{b}	21.97 ± 2.31^{b}
Neutrophils (%)	17.48 ± 3.78^{c}	8.33 ± 1.70^{a}	9.67 ± 0.47^{a}	13.50 ± 1.73^{b}	9.33 ± 0.94^{a}
Lymphocytes (%)	74.50 ± 3.79^{c}	82.33 ± 2.05^{a}	82.33 ± 1.05^{c}	78.33 ± 2.36^{b}	85.00 ± 0.00^{c}
Monocytes (%)	8.33 ± 0.47^{b}	9.33 ± 0.47^{c}	8.00 ± 0.82^{b}	5.00 ± 0.00^{a}	5.67 ± 0.94^{a}

Note: C+: 10% iodine; C-: Ointment base; LPC6: Liposome ointment of 6% red betel extract; LPC9: 9% red betel extract liposome ointment; and LPC12: 12% red betel extract liposome ointment. Data were presented in the form of mean ± standard deviation (SD) Statistical analysis used one-way ANOVA followed by the Duncan Multiple Range Test (DMRT ($p < 0.05$).

Although the negative control group (base ointment) showed the highest platelets (209.11 ± 224.98 ×10^3/μL), these values were not in line with improved wound healing outcomes, indicating that platelet levels must be interpreted alongside other hematological parameters. MCV values in LPC9 and LPC12 were 42.33 ± 0.047 fL and 46.63 ± 4.31 fL, respectively, while MCH in LPC6 reached 17.67 ± 2.67 pg, indicating erythrocyte qualities that support oxygen transport. The distributing of while blood cells also showed important differences, with neutrophil and lymphocyte percentages in the LPC9 group at 13.50 ± 1.73% and 78.33 ± 2.36%, respectively, suggesting a controlled inflammatory phase and timely transision to the proliferation phase that support healing. Overall, these data indicate that the 9% red betel extract liposome ointment is the most effective concentration in modulating the immune and hematological response to accelerate wound healing in mice, as supported by statistical analysis ($p < 0.05$). The liposomal formulation increases the bioavailability of active compounds in red betel extract, providing anti-inflammatory effect while stimulating optimal tissue regeneration.

Changes in blood profile often occur as a result of viral and bacterial infections. Severe infections can damage endothelial cells and cause red blood cell rupture (erythrolysis), leading to reduced oxygen and nutrient delivery to tissues. As a result, the bone marrow works harder but produces pink blood cells (reticulocytes) with low hemoglobin levels, resulting in reduced ability to carry oxygen [72]. The flavonoids present in *Piper crocatum* may inhibit the transcription pathway of NF-κB factor, which regulates the expression of proinflammatory cytokines such as TNF-

α, IL-1β, and IL-6 [73,74]. This mechanism reduces inflammation and oxidative damage to blood elements, such as erythrocytes and platelets during inflammation, thus maintaining the homeostasis of the blood profile. In addition, it also inhibits the COX and lipooxygenase pathways as well as the work of TACE, thereby effectively reducing the secretion of proinflammatory cytokines [75]. Furthermore, studies have shown improved bone consistency and reduced swelling in a mouse model of arthritis, indicating the strong anti-inflammatory activity of the flavonoids. Furthermore, the combination of significant phenolic and flavonoid levels in *Piper crocatum* provides synergistic antioxidant effects, helps neutralize free radicals produced during inflammation and maintains stability in the number of leukocytes, hemoglobin, hematocrit, and platelet levels. Flavonoids protect blood cells from oxidative stress, prevent erythrocyte hemolysis, inhibit platelet aggregation (thereby exerting antithrombotic effects), and suppress leukocyte activation that triggers inflammation [76]. This effect supports wound healing through modulation of the immune response and blood hemostasis, thereby maintaining optimal blood cell function during wound tissue repair. The phenolic and flavonoid levels of red betel leaf extract (*Piper crocatum*) in this study were 496.10 ± 1.08 μg GAE/g and 644.44 ± 48.11 μg QE/g extract, respectively. These values indicate a relatively high content of phenolic compounds and flavonoids, which may contribute to its biological activity [77].

Improvement in blood parameters typically occurs as the inflammatory process subsides and healing progresses. Inflammation is a complex physiological response to damage or infection, which goes through several phases, including hemostasis (blood clotting), acute inflammation, proliferation of new tissues, and tissue remodeling [78]. In the inflammatory phase, there is activation and migration of immune cells such as leukocytes to the site of damage or infection, accompanied by changes in blood parameters that reflect immune activity and healing processes. As inflammation diminishes, the proliferation and remodeling phases predominate, leading to a decrease in the number of active inflammatory cells in the tissues. The production of red blood cells (erythrocytes), hemoglobin, platelets return to normal, and the distribution of blood cells that were previously disrupted gradually improves. Consequently, leukocytes, erythrocytes, hemoglobin, hematocrit, platelets, MCV, MCH, RDW, neutrophils, lymphocytes, and monocytes return to normal ranges [79]. In chronic wounds, the epidermis shows hyperproliferation without the ability to migrate, unresolved inflammation, and infection associated with biofilm formation. Although inflammatory cells such as neutrophils and macrophages are increased, their function is impaired. Uncontrolled proteases disrupt important repair mechanisms, and many fibroblasts undergo senescence. In chronic wounds, angiogenesis, stem cell recruitment and activation, and ECM remodeling decreased when compared to normal wound healing processes [71].

This repair not only occurs naturally, but can also be accelerated and supported by the topical application of natural ingredients with anti-inflammatory and wound healing properties [80]. Active compounds in topical natural ingredients can help inhibit inflammatory mediators, stimulate cell proliferation, and promote tissue regeneration, thereby accelerating the resolution of inflammation and facilitating faster normalization of blood parameters.

Conclusion

Apigenin, a compound recommended as a candidate for skin wound treatment from red betel leaves, demonstrates favorable physicochemical properties, PA value, pharmacokinetics, toxicity, binding affinity, and amino acid residues. Based on these parameters, apigenin shows superior performance compared with eugenol and tetrahydrocurcumin, as well as control drugs in the inflammatory pathway (celecoxib) and estrogen pathway (estradiol and finasteride), particularly in the relation to cyclooxygenase-2 (COX-2) and estrogen receptor alpha (ER-α/IR5K) and beta (ER-β/1X7B).

Furthermore, all ointments, including controls, have a stable semi-solid texture, pH accordingly, and good dispersion. The red betel liposome (LPC) formula shows physical stability, no rancid odor, and emollient-occlusive properties. Increased LPC levels affect the color of the preparation and increase anti-inflammatory activity through modulation of inflammatory mediators and protection against oxidative stress. Based on the results, LPC9 showed the highest physical stability, while LPC12 is recommended due to its superior effect

on wound healing and blood profile improvement.

Acknowledgment

Internal Research of the Faculty of Mathematics and Natural Sciences, State University of Malang Jawa Timur 65145, Indonesia No. 24.2.83/UN32.3/LT/2025).

Conflict of Interest

This study has no conflicts of interest.

Declaration of Generative AI in Scientific Writing

The authors declare that no generative AI tools were used in this current study.

CRediT Author Statement

Siti Imroatul Maslikah: Conceptualization, Supervision, Methodology, Formal analysis, Validation, Project administration, and Writing original draft. **Wira Eka Putra**: Supervision, Methodology, Formal analysis, Validation, Visualization, and Writing original draft. **Sri Rahayu Lestari**: Supervision, Methodology, Formal analysis, Validation, and Writing review & editing. **Ajeng Daniarsih**: Supervision, Methodology, Formal analysis, Validation, and Writing review & editing. **Agung Witjoro**: Supervision, Methodology, Formal analysis, Validation, and Writing review & editing. **Alif Baroroh**: Methodology, Investigation, Validation, Visualization, and Writing review & editing. **Nur Laila**: Methodology, Investigation, Visualization, and Writing review & editing. **Eka Desi Lilin Yuliani**: Methodology, Investigation, Visualization, and Writing review & editing.

References

[1] Naziyah, R Hidayat and Maulidya. Penyuluhan manajemen luka terkini dalam situasi pandemic Covid -19 melalui kegiatan pesantren luka dengan menggunakan media zoom meeting bagi mahasiswa prodi keperawatan & profesi ners fakultas ilmu kesehatan Universitas Nasional Jakarta. *Jurnal Kreativitas Pengabdian Kepada Masyarakat (PKM)* 2022; **5(7)**, 2061-2070.

[2] MN Djuddawi and ANH Kholidha. Test effectiveness of genegrass (*Cymbopogon citratus*) against the healing of wounds in white mice. *Journal of Professional Care Research* 2019; **5(1)**, 13-21.

[3] M Al-Musawi, SH Turki, H Al-Naymi, SS Al-Salman, VV Boroujeni, M Alizadeh, M Sattar, F Sharifianjazi, L Bazli, AMD Pajooh, M Shahriari-Khalaji, A Najafinezhad, FM Moghadam, M Mirhaj and M Tavakoli. Localized delivery of healing stimulator medicines for enhanced wound treatment. *Journal of Drug Delivery Science and Technology* 2024; **101**, 106212.

[4] W Wang, KJ Lu, CH Yu, QL Huang and Y Du. Nano-drug delivery systems in wound treatment and skin regeneration. *Journal of Nanobiotechnology* 2019; **17**, 82.

[5] DL Gbian and A Omri. Lipid-based drug delivery systems for disease managements. *Biomedicines* 2022; **10(9)**, 2137.

[6] S Hallaj-Nezhadi and M Hassan. Nanoliposome-based antibacterial drug delivery. *Drug Delivery* 2015; **22(5)**, 581-589.

[7] E Wardani and RA Rachmania. Activity test of ethanol extract and ethyl acetate extract of red betel leaf (*Piper cf. fragile*) on the healing of open wounds in rats. *Pharmaceutical Media: Journal of Pharmaceutical Sciences* 2017; **14(1)**, 43.

[8] F Ulviani, Y Yusriadi and K Khaerati. Effect of red betel leaf extract gel (*Piper crocatum* Ruiz & Pav) on burn healing in rabbits (*Oryctolagus cuniculus*). *Galenika Journal of Pharmacy* 2016; **2(2)**, 103-110.

[9] Febriyenti, DP Putra, EI Wicaksanti and CD Hamami. Formulasi liposom ekstrak terpurifikasi centella asiatica menggunakan fosfatidilkolin dan kolesterol. *Jurnal Sains Farmasi & Klinis* 2018; **5(2)**, 78-82.

[10] Amrianto, Mukarramah, DD Sukmana, N Nahda and AD Permana. Formulasi ekstrak buah mengkudu (*Morinda citrifolia*) dalam bentuk sediaan transdermal liposome cream. *Proceedings of the National Seminar on Biology for Life Gowa* 2017; **3(1)**, 19-25.

[11] AD Rizkita, E Cahyono and S Mursiti. Isolasi dan uji antibakteri minyak daun sirih hijau dan merah terhadap Streptococcus mutans. *Indonesian Journal of Chemical Science* 2017; **6(3)**, 279-286.

[12] P Barazesh, H Hajihassani, F Motalebi, SMH Neiresi, R Hajihassani and AR Mehrabian. Unlocking the healing potential: A comprehensive review of ecology and biology of medical-grade

honey in wound management and tissue regeneration. *Health Science Reports* 2025; **8**, e70240.

[13] RAZ Aziz and ER Purnama. *In silico* analysis of the potential of red betel (*Piper crocatum*) active compounds as anti-inflammatory drug candidate. *Journal of Universitas Negeri Surabaya* 2024; **13(3)**, 382-392.

[14] SI Maslikah and WE Putra. Molecular dynamics simulation of various bioactive compounds of red betel (*Piper crocatum*) as anti-inflammatory drug-like candidates in rheumatoid arthritis treatment. *Trends in Sciences* 2024; **21(3)**, 7334.

[15] AB Umar, A Uzairu, GA Shallangwa and S Uba. *In silico* evaluation of some 4-(quinolin-2-yl)pyrimidin-2-amine derivatives as potent V600E-BRAF inhibitors with pharmacokinetics, ADMET, and drug-likeness predictions. *Future Journal of Pharmaceutical Sciences* 2020; **6**, 61.

[16] HTT Trang, NX Ha, CH Le, TTT Nhung, DTT Giang, NTD Hang and PT Thuy. *In silico* molecular docking, DFT, and toxicity studies of potential inhibitors derived from *Millettia dielsiana* against human inducible nitric oxide synthase. *Journal of Chemical Research* 2024. https://doi.org/10.1177/17475198241263837

[17] FB Lopes, MM Sarandy, RD Novaes, G Valacchi and RV Gonçalves. OxInflammatory responses in the wound healing process: A systematic review. *Antioxidants* 2024; **13(7)**, 823.

[18] MM Guardado, V Lutz, M Hengstschläger and H Dolznig. The role of prostaglandins as major inflammatory mediators in colorectal cancer. *International Journal of Molecular Sciences* 2025; **26(24)**, 12191.

[19] F Akbari, M Azadbakht, A Bagheri and L Vahedi. *In silico*, *in vitro*, and *in vivo* wound healing activity of *Astragalus microcephalus* willd. *Advances in Pharmacological and Pharmaceutical Sciences* 2022; **2022**, 2156629.

[20] MI Ahamed, SI Mim and MMI Emu. *In silico* functional annotation of E2102 hypothetical protein from *Aeromonas veronii*. *Genetics of Aquatic Organisms* 2025; **9(2)**, GA884.

[21] W Masocha and MA Khedr. Correlation between *in silico* docking/simulation results and *in vitro* MAGL inhibition potency of selected triterpenes. *Current Issues in Molecular Biology* 2025; **47(9)**, 691.

[22] Fatimawali, MJ Kalalo, SB Simanjuntak, TA Hebber, BJ Kepel and TE Tallei. Immunomodulatory potential of bioactive compounds of betel leaf extract targeting COVID-19 immunological human host proteins: An *in silico* study. *Journal of Applied Pharmaceutical Science* 2022; **12(2)**, 75-88.

[23] M Khalil. Simulasi *Molecular docking* senyawa coumestrol dengan protein kapsid virus hepatitis B: Studi *in silico* potensi senyawa alami. *Jurnal Jeumpa* 2023; **10(1)**, 138-148.

[24] K Gabriel, NN Hidayat, FA Khaerani and PE Gaharani. Studi *in silico* senyawa metabolit sekunder daun kenikir (Cosmos Caudatus Kunth.) sebagai antikanker ovarium terhadap ESR-1. *Indonesian Journal of Mathematics and Natural Sciences* 2024; **47(2)**, 85-98.

[25] SR Rena, Nurhidayah and Rustan. Analisis molecular docking senyawa Garcinia mangostana L. sebagai kandidat anti SARS-CoV-2. *Jurnal Fisika Unand* 2022; **11(1)**, 82-88.

[26] KA Nofianti, L Hakim, Suzana and F Ifadotunikamah. Prediction of the potential of benzoxazinone, 2-phenyl-4H-benzo[1,3]oxazin-4-one, and 2-[2-(4-methoxyphenyl)vinyl]-3,1-benzoxazin-4-one as new anti-tuberculosis agents. *Berkala Ilmiah Kimia Farmasi* 2024; **11(1)**, 26-32.

[27] ASH Hoseini, A Mohebshahedin, S Ghiabi, M KhalatbariLimaki, M Arastonejad, S Hassani, M Alem and ER Basmenj. ADMET, QSAR and docking studies to predict the activity of *tyrosinase*-derived medication inhibitors based on computational techniques. *Current Research in Structural Biology* 2025; **10**, 100174.

[28] A Pramudiyawati, DE Putri, Nurfadilah and A Wilapangga. Skrining studi *in silico* potensi farmakokinetika dan toksisitas senyawa 6,10,14-trimetil-2-pentadekanon dari ekstrak daun ekaliptus. *Indonesian Journal of Pharmaceutical Education* 2024; **4(1)**, 39-46.

[29] A Wilapangga, B Sutyono, T Permadi and ER Noordam. Potensi farmakokinetika dan toksisitas *Benzyl β-D-Glucoside* dari *Piper crocatum*: Studi *in silico*. *Journal Syifa Sciences and Clinical Research* 2024; **6(2)**, 173-180.

[30] N Mukhopadhyay, A Shukla, PN Makhal and VR Kaki. Natural product-driven dual COX-LOX inhibitors: Overview of recent studies on the development of novel anti-inflammatory agents. *Heliyon* 2023; **9(3)**, e14569.

[31] IM Comino-Sanz, MD López-Franco, B Castro and PL Pancorbo-Hidalgo. The role of antioxidants on wound healing: A review of the current evidence. *Journal of Clinical Medicine* 2021; **10(16)**, 3558.

[32] CC Voda, IA Stefanopol, G Gurau, MA Hîncu, GV Popa, OG Mateescu, L Baroiu and MC Mehedinti. Update on the study of angiogenesis in surgical wounds in patients with childhood obesity. *Biomedicines* 2025; **13(2)**, 375.

[33] SO Oselusi, NRS Sibuyi, DR Martin, M Meyer and AM Madiehe. Potential matrix metalloproteinase 2 and 9 inhibitors identified from *Ehretia* species for the treatment of chronic wounds: Computational drug discovery approaches. *Computers in Biology and Medicine* 2025; **185**, 109487.

[34] ZFK Al-Zubaidy and MT Naqi. The effect lanolin extract and vaseline with glycerine mixture to treatment by affecting of IL-4 and IL-13 level in induced eczema in rats. *International Journal of Health Sciences* 2022; **6**, 1606-1612.

[35] YC Cheng, TS Li, HL Su, PC Lee and HMD Wang. Transdermal delivery systems of natural products applied to skin therapy and care. *Molecules* 2020; **25(21)**, 5051.

[36] L Farias, CB Pereira, G Machado, C Schmidt and AC de Vargas. Stability evaluation of propolis topical bases for veterinary use. *Brazilian Archives of Biology and Technology* 2013; **56(6)**, 942-947.

[37] L Coderch, L Ricci, M Martí, S Bagherpour, L Pérez-García and C Alonso. Liposomal formulations for waterproofing mucosal membranes. *European Journal of Pharmaceutics and Biopharmaceutics* 2025; **213**, 114757.

[38] N Lely, Dachriyanus, Y Aldi, Almahdy and FS Wahyuni. Anti-inflammatory effect of isolate compounds from ethyl acetate fraction of *Piper crocatum* Ruiz and Pav leaves on lipopolysaccharide-induced RAW 264.7 cells. *HAYATI Journal of Biosciences* 2023; **30(1)**, 28-34.

[39] NM Aisyiyah, KAAK Siregar and PM Kustiawan. Review: Potential of red betel leaves (*Piper crocatum*) as anti-inflammatory in *Rheumatoid arthritis*. *Jurnal Farmasi Sains dan Praktis* 2021; **7(2)**, 197-206.

[40] P Ghosha, NK Brogdena and AL Stinchcomb. Effect of formulation pH on transport of naltrexone species and pore closure in microneedle-enhanced transdermal drug delivery. *Molecular Pharmaceutics* 2013; **10(6)**, 2331-2339.

[41] S Megawati. Formulation and effectiveness of wound healing of methanol extract of *Thevetia peruviana* on New Zealand white male rabbits. *Udayana Pharmacy Journal* 2020; **9(3)**, 180.

[42] JY Hernawan, H Kurniawan and AP Lestari. Stability test of salep extract white garlic (*Alliumsativum*) with vaselin album base. *Journal Permata Indonesia* 2020; **11(1)**, 11-15.

[43] VH Damanik, L Pratiwi and B Wijianto. Formulasi NLC-Stick ekstrak bunga telang (*Clitoria ternatea* L.) dengan variasi konsentrasi shea butter dan asam stearat. *Indonesian Journal of Pharmaceutical and Clinical Research* 2024; **7(1)**, 16-21.

[44] JS Buratto, CHDS Fernandes, JCG Rosa, ATDF Vanzo and JH Caviglione. Use of quantitative colorimetry and visual evaluation for color characterization of triticale seeds after phenol reaction. *Journal of Seed Science* 2021; **43**, e202143008.

[45] B Milovanovic, I Djekic, J Miocinovic, V Djordjevic, JM Lorenzo, FJ Barba, D Mörlein and I Tomasevic. What is the color of milk and dairy products and How is it Measured? *Foods* 2020; **9(11)**, 1629.

[46] S Ropciuc, C Ghinea, A Leahu, AE Prisacaru, MA Oroian, LC Apostol and F Dranca. Development and characterization of new plant-based ice cream assortments using oleogels as fat source. *Gels* 2024; **10(6)**, 397.

[47] I Maesaroh, D Pratiwi and L Agustin. Ointment formulation and test preparation from *Manilkara zapota* L. leaf extract using variation of ointment

base as boils. *Indonesian Journal of Pharmaceutics* 2020; **2(1)**, 14-19.

[48] MN Calienni, LM Martínez, MC Izquierdo, SDV Alonso and J Montanari. Rheological and viscoelastic analysis of hybrid formulations for topical application. *Pharmaceutics* 2023; **15(10)**, 2392.

[49] M Piechota-Urbańska, J Kołodziejska and MM Zgoda. Viscosity of pharmacopeial multimolecular ointment vehicles and pharmaceutical availability of a model therapeutic agent. *Polymers in Medicine* 2007; **37(2)**, 3-19.

[50] K Lis. Hypersensitivity to lanolin: An old–new problem. *Life* 2024; **14(12)**, 1553.

[51] W Weyenberg, P Sollie and A Ludwig. Influence of the concentrations of liposomes and a submicron emulsion on the rheological properties of a topical gel. *Pharmazie* 2006; **61(11)**, 938-942.

[52] KT Keylock, VJ Vieira, MA Wallig, LA DiPietro, M Schrementi and JA Woods. Exercise accelerates cutaneous wound healing and decreases wound inflammation in aged mice. *American Journal of Physiology - Regulatory Integrative and Comparative Physiology* 2008; **294(1)**, 179-184.

[53] J Hajj, B Sizemore and K Singh. Impact of epigenetics, diet, and nutrition-related pathologies on wound healing. 2024; **25(19)**, 10474.

[54] I Seth, B Lim, J Cevik, D Gracias, M Chua, PS Kenney, WM Rozen and R Cuomo. Impact of nutrition on skin wound healing and aesthetic outcomes: A comprehensive narrative review. *JPRAS Open* 2024; **39**, 291-302.

[55] SG G/Giorgis, D Ambikar, A Tsegaw and YM Belayneh. Wound healing activity of 80% methanolic crude extract and solvent fractions of the leaves of *Justicia schimperiana* (Hochst. ex Nees) T. Anderson (Acanthaceae) in mice. *Journal of Experimental Pharmacology* 2022; **14**, 167-183.

[56] R Mare, S Maurotti, Y Ferro, A Galluccio, F Arturi, S Romeo, A Procopio, V Musolino, V Mollace, T Montalcini and A Pujia. A rapid and cheap method for extracting and quantifying lycopene content in tomato sauces: Effects of lycopene micellar delivery on human osteoblast-like cells. *Nutrients* 2022; **14(3)**, 717.

[57] S Hanbisa, WT Tadesse and T Abula. Evaluation of wound healing activity of 80% methanol stem-bark extract and solvent fractions of *Prunus africana* (*Hook.f.*) *Kalkman* (Rosaceae) in mice. *Journal of Experimental Pharmacology* 2023; **15**, 349-365.

[58] P Diaz, SC Jeong, S Lee, C Khoo and SR Koyyalamudi. Antioxidant and anti-inflammatory activities of selected medicinal plants and fungi containing phenolic and flavonoid compounds. *Chinese Medicine* 2012; **7**, 26.

[59] AK Shrivastava, M Keshari, M Neupane, S Chaudhary, PK Dhakal, L Shrestha, A Palikhey, CK Yadav, G Lamichhane, MU Shekh and RK Yadav. Evaluation of antioxidant and anti-inflammatory activities, and metabolite profiling of selected medicinal plants of Nepal. *Journal of Tropical Medicine* 2023; **2023**, 6641018.

[60] N Zulkefli, CNMC Zahari, NH Sayuti, AA Kamarudin, N Saad, HS Hamezah, H Bunawan, SN Baharum, A Mediani, QU Ahmed, AEH Ismail and MN Sarian. Flavonoids as potential wound-healing molecules: Emphasis on pathways perspective. *International Journal of Molecular Sciences* 2023; **24(5)**, 4607.

[61] JM Al-Khayri, GR Sahana, P Nagella, BV Joseph, FM Alessa and MQ Al-Mssallem. Flavonoids as potential anti-inflammatory molecules: A review. *Molecules* 2022; **27(9)**, 2901.

[62] P Pandey, S Lakhanpa, D Mahmood, HN Kang, B Kim, S Kang, J Choi, M Choi, S Pandey, M Bhat, S Sharma, F Khan, MN Park and B Kim. An updated review summarizing the anticancer potential of flavonoids via targeting NF-kB pathway. *Frontier in Pharmacology* 2025; **15**, 1513422.

[63] A Sychrová, G Škovranová, M Čulenová and SB Fialová. Prenylated flavonoids in topical infections and wound healing. *Molecules* 2022; **27(14)**, 4491.

[64] Y Gong, HX Li, RH Guo, W Widowati, YH Kim, SY Yang and YR Kim. Anti-allergic inflammatory components from the leaves of *Piper crocatum* Ruiz & Pav. *Biological and Pharmaceutical Bulletin* 2021; **44(2)**, 245-250.

[65] M Cedillo-Cortezano, LR Martinez-Cuevas, JAM López, ILB López, S Escutia-Perez and VL

Petricevich. Use of medicinal plants in the process of wound healing: A literature review. *Pharmaceuticals* 2024; **17(3)**, 303.

[66] L Sercombe, T Veerati, F Moheimani, SY Wu, AK Sood and S Hua. Advances and challenges of liposome assisted drug delivery. *Frontiers in Pharmacology* 2015; **6**, 00286.

[67] INE Lister, CN Ginting, E Girsang, A Armansyah, HH Marpaung, APF Sinaga, RAS Handayani and R Rizal. Antioxidant properties of red betel (*Piper crocatum*) leaf extract and its compounds. *Journal of Natural Remedies* 2019; **19(4)**, 198-205.

[68] A Borges, MLM Calvo, JA Vaz and RC Calhelha. Enhancing wound healing: A comprehensive review of sericin and *Chelidonium majus* L. as potential dressings. *Materials* 2024; **17(17)**, 4199.

[69] SA Eming, T Krieg and JM Davidson. Inflammation in wound repair: Molecular and cellular mechanisms. *Journal of Investigative Dermatology* 2007; **127(3)**, 514-525.

[70] J Irma, AS Kartasasmita, A Kartiwa, I Irfani, SA Rizki and S Onasis. From growth factors to structure: PDGF and TGF-β in granulation tissue formation: A literature review. *Journal of Cellular and Molecular Medicine* 2025; **29(11)**, e70374.

[71] SA Eming, P Martin and M Tomic-Canic. Wound repair and regeneration: Mechanisms, signaling, and translation. *Science Translational Medicine* 2016; **6(265)**, 265sr6.

[72] YA Prakoso, N Hidayah, CS Rini and Kurniasih. Dynamic change of blood profile in rat models with acute skin injury artificially infected with methicillin-resistant *Staphylococcus aureus*. *Veterinary World* 2021; **14(8)**, 2085-2090.

[73] DR Laksmitawati, A Widyastuti, N Karami, E Afifah, DD Rihibiha, H Nufus and W Widowati. Anti-inflammatory effects of *Anredera cordifolia* and *Piper crocatum* extracts on lipopolysaccharide-stimulated macrophage cell line. *Bangladesh Journal of Pharmacology* 2017; **12**, 35-40.

[74] INE Lister, CN Ginting, E Girsang, ED Nataya, AM Azizah and W Widowati. Hepatoprotective properties of red betel (*Piper crocatum* Ruiz and Pav) leaves extract towards H_2O_2-induced HepG2 cells via anti-inflammatory, antinecrotic, antioxidant potency. *Saudi Pharmaceutical Journal* 2020; **28(10)**, 1182-1189.

[75] M Rispandi, NS Harahap and R Mediyana. The potential of red betel leaf essential oil (*Piper crocatum* Ruiz & Pav) as an anti-bleeding in the management of coronavirus infection. *NeuroQuantology* 2023; **21(1)**, 381-387.

[76] S Asgary, G Naderi and N Askari. Protective effect of flavonoids against red blood cell hemolysis by free radicals. *Experimental and Clinical Cardiology* 2005; **10(2)**, 88-90.

[77] SI Maslikah, SR Lestari, S Siri, M Yunus, AR El-Baroroh, DS Miasih, M Rifa'i, Warsito and MS Djati. Phytochemical screening and antioxidant potential of ethanol extract from *Piper crocatum* leaves. *Tropical Journal of Natural Product Research* 2025; **9(7)**, 3114-3119.

[78] S Singh, A Young and CE McNaught. The physiology of wound healing. *Surgery* 2017; **35(9)**, 473-477.

[79] L Cañedo-Dorantes and M Cañedo-Ayala. Skin acute wound healing: A comprehensive review. *International Journal of Inflammation* 2019; **2019(1)**, 3706315.

[80] RA El-Shiekh, MH Radi, R Elshimy, E Abdel-Sattar, AM El-Halawany, MA Ibrahim, ME Ali and EI Hassanen. Friedelin: A natural compound exhibited potent antibacterial, anti-inflammatory, and wound healing properties against MRSA-infected wounds. *Naunyn-Schmiedeberg's Archives of Pharmacology* 2025; **398(9)**, 12103-12113.